DOCTORAL DISSERTATION SERIES

TITLE ANALYSIS OF FUEL SPRAYS BY ELECTRICAL METHODS

AUTHOR IBRAHIM H. A. ELABD

UNIVERSITY OF MICH. DATE 1950

DEGREE Sc. D. PUBLICATION NO. 2399



UNIVERSITY MICROFILMS
ANN ARBOR · MICHIGAN

ANALYSIS OF FUEL SPRAYS BY ELECTRICAL METHODS

by
Ibrahim H. A. Elabd

A dissertation submitted in partial fulfillment
of the requirements for the degree of
Doctor of Science in the
University of Michigan
1950

Committee in charge:

Professor L. N. Holland, Chairman
Professor S. S. Attwood
Asst. Prof. N. Coburn
Professor W. G. Dow
Assoc. Prof. W. W. Hagerty
Professor M. B. Stout

ACKNOWLEDGEMENTS

I should like to express my sincere thanks to many people for the kind assistance and encouragement rendered to me during the course of this work.

Professor L. N. Holland, chairman of the doctoral committee, was especially helpful in his expert guidance and assistance.

I am also very grateful to Professors S. S. Attwood, N. Coburn, W. G. Dow, W. W. Hagerty, and M. B. Stout, the remaining members of the committee, for their helpful co-operation.

Much practical assistance was supplied by the Engineering Research Institute's Spray Project which is headed by Professor R. A. Dodge. Mr. Raymond Yagle and Mr. Milo Kaufman also rendered help in experimental construction and operation.

Special thanks go to the Air Materiel Command of the United States Air Forces for permission to use equipment designed and built for their research.

TABLE OF CONTENTS

	Page
INTRODUCTION	1
CHAPTER I: STRAIN GAUGE ANALYZER	4
Theory	4
Apparatus	9
Results	15
Discussion of Results	28
CHAPTER II: TUBE ANALYZER	31
Theory	31
Apparatus	35
Results	39
Discussion of Results	44
CHAPTER III: OTHER METHODS	56
Absorption of Light	56
Radioactivity	58
Capacitance	59
CONCLUSIONS	64
APPENDIX I: SAMPLE OF CALCULATIONS	68
APPENDIX II: EXACT CALCULATION OF FORCE IN SPRAY	71
APPENDIX III: SENSITIVITY OF TWO TUBES COMPARED TO ONE TUBE	80
APPENDIX IV: HISTORIC SURVEY OF SPRAY ANALYZERS	83
BIBLIOGRAPHY	86
PICTURES	91

LIST OF TABLES

		Page
1.	Data on Spray of Nozzle 6702074 A 4-2/3 DED C52 (Strain Gauge)	16
2.	Data on Spray of Nozzle 6702074 A 4-2/3 DED C52 (Strain Gauge)	17
3.	Data on Spray of Nozzle 6702074 A 4-2/3 DED C52 (Strain Gauge)	18
4.	Calibration of the One Tube Arrangement	40
5.	Calibration of the Two Tube Arrangement	42
6.	Data on Spray of Nozzle 6702074 A 4-2/3 DED C52 (One Tube)	46
7.	Data on Spray of Nozzle 6702074 A 4-2/3 DED C52 (One Tube)	47
8.	Data on Spray of Nozzle 6702074 A 4-2/3 DED C52 (One Tube)	48
9.	Data on Spray of Nozzle 6702074 A 4-2/3 DED C52 (One Tube)	49

LIST OF ILLUSTRATIONS

		Page
1.	Dimensions of Cantilevered Beam	5
2.	(a) Position of Equilibrium of Cantilevered Beam (b) Impact Between Sheath and Wire	6 6
3.	Block Diagram of Strain Analyzer	10
4.	Circuit Diagram of Strain Analyzer	11
5.	Mercury Slip Rings Set Up	13
6.	Circuit Diagram of Brush Oscillograph	13
7.	Osicllograph Chart for Simplex Nozzle 6702074 A 4-2/3 DED C52 (Strain Gauge 100 PSI)	19
8.	Oscillograph Chart for Simplex Nozzle 6702074 A 4-2/3 DED C52 (Strain Gauge 200 PSI)	20
9.	Oscillograph Chart for Simplex Nozzle 6702074 A 4-2/3 DED C52 (Strain Gauge 300 PSI)	21
10.	Oscillograph Chart for Defaced Simplex Nozzle 6702074 A 3-29-48 5 DED C52 (Strain Gauge 100 PSI)	22
11.	Oscillograph Chart for Defaced Simplex Nozzle 6702074 A 3-29-48 5 DED C52 (Strain Gauge 200 PSI)	23
12.	Oscillograph Chart for Defaced Simplex Nozzle 6702074 A 3-29-48 5 DED C52 (Strain Gauge 300 PSI)	24
13.	Oscillograph Chart for Defaced (but improved) Simplex Nozzle 6702074 A 3-29-48 5 DED C52 (Strain Gauge 100 PSI)	25
14.	Oscillograph Chart for Simplex Nozzle 6702074 A 4-2/3 DED C52 with 1/16" Wire Inserted in the Spray (Strain Gauge 200 PSI)	26
15.	Oscillograph Chart for Defaced Simplex Nozzle 6702074 A 3-29-48 5 DED C52 Using a 500 u.f. Condenser Across Amplifier (Strain Gauge 200 PSI)	27
16.	Variation of Sheath Thickness of Simplex Nozzle With Pressure	30
17.	Schematic Diagram of the RCA 5734 Mechano-Electronic Transducer	32

		Page
18.	Position of Equilibrium of Tube Arm	32
19.	Connection Diagram for Tube Analyzer	36
20.	Circuit Diagram of Brush d-c Amplifier	37
21.	Calibration Curve for One Tube	41
22.	Calibration Curve for Two Tubes	43
23.	Oscillograph Chart for Simplex Nozzle 6702074 A 4-2/3 DED C52 (Tube 200 PSI)	50
24.	Oscillograph Chart for Simplex Nozzle 6702074 A 4-2/3 DED C52 (Tube 400 PSI)	51
25.	Oscillograph Chart for Simplex Nozzle 6702074 A 4-2/3 DED C52 (Tube 500 PSI)	52
26.	Oscillograph Chart for Defaced Nozzle 6702074 A 3-29-48 5 DED C52 (Tube 200 PSI)	53
27.	Oscillograph Chart for Simplex Nozzle 5230410 122A Using a 4 u.f. Condenser Across Amplifier Input (Tube 50 PSI)	54
28.	Oscillograph Chart for Simplex Nozzle 5230410 93A Using a 4 u.f. Condenser Across Amplifier Input (Tube 75 PSI)	55

LIST OF PICTURES

		Page
1.	Flow of Typical Simplex Nozzle (25 PSI)	91
2.	Flow of Typical Simplex Nozzle (50 PSI)	91
3.	Flow of Typical Simplex Nozzle (75 PSI)	92
4.	Flow of Typical Simplex Nozzle (100 PSI)	92
5.	Flow of Typical Simplex Nozzle (200 PSI)	93
6.	Flow of Typical Simplex Nozzle (300 PSI)	93
7.	Flow of Typical Simplex Nozzle (400 PSI)	94
8.	Flow of Typical Simplex Nozzle (500 PSI)	94
9.	Slender Cupro Nickel Wire Pick Up (50 PSI)	95
10.	Slender Cupro Nickel Wire Pick Up (25 PSI)	95
11.	Orifice of Defaced Simplex Nozzle	96
12.	Flow of Defaced Simplex Nozzle (50 PSI)	97
13.	Flow of Defaced Simplex Nozzle (100 PSI)	97
14	Bracket Carrying Cantilevered Beam	98
15.	Mounting of Strain Gauge Pick Up	98
16.	Meter Panel and Spray Chamber	99
17.	Piping System Between Pumps and Nozzle	100
18.	Mounting of One Tube	101
19.	Mounting of Two Tubes	102

INTRODUCTION

The use of jet propelled aircraft has increased to a very large extent in the few years since their introduction to the aeronautics industry. During this time, the jet airplane has progressed from an experimental and dangerous aircraft to its present status as an accepted and useful type of plane which is becoming a common sight in the air.

The increasing use of jet engines, however, has emphasized the need for efficient fuel spray testing equipment for the nozzles used in their combustion chambers. It has been ascertained that a jet engine can function satisfactorily only if the nozzles introducing the fuel into the combustion chambers yield uniform sprays under a wide variety of operating conditions.

It is the purpose of this work to devise various methods for testing nozzles and analyzing fuel sprays. This is of prime importance in mass production operations where large numbers of nozzles must be calibrated accurately and rapidly. An ideal fuel spray analyzer should:

1. Survey the spray rapidly for uniformity
2. Give quantitative information about the mass distribution of the spray around the spray cone, point by point, and indicate mean drop size.
3. Be compact enough to be installed in the combustion chamber so that it can give the required spray information under the actual fuel flow conditions.

4. Not interfere with the actual air-fuel flow.
5. Determine to what extent each nozzle of any set is matched against the others at all fuel pressures.
6. Yield permanent graphical records which can easily be compared with those of a standard reference nozzle.

Previously, experimentation on this problem has been confined to the study of the mean size and distribution of the drops of fuel emanating from the nozzle. Several methods were developed for the study of the droplet size and distribution; these are described in the historical survey of the problem included in Appendix IV.

However, all these methods are elaborate, expensive, and time consuming, and a quicker method of testing nozzles for industrial use was sought. In a closed conference on fuel sprays held at the University of Michigan in March, 1949, it was agreed that a study of the conical sheath of liquid fuel in the direct vicinity of the nozzle, before the liquid disintegrates into drops, would yield sufficient knowledge of the spray characteristics to evaluate nozzle performance. Since that date, therefore, the author has confined his work to a study of the behavior of these conical sheaths. Two different means, one using a strain gauge and the other using the RCA tube No. 5734 as a pick up, were finally devised by which the sheath thickness and the circumferential uniformity of the spray cone can be studied quickly and accurately. It is believed that these

methods approach the ideal analyzer previously described as closely as can be achieved at present.

CHAPTER I

STRAIN GAUGE ANALYZER

Theory:

The purpose of this method is to find the thickness of the conical sheath of the fuel spray in the direct vicinity of the nozzle. This is accomplished by using electric strain gauges to measure the force of the impact of the spray upon a cantilevered beam. The beam is simply a thin sheet of phosphor bronze .01 inch thick fixed at one end; to its free end is attached a wire 1/16 inches diameter. The dimensions of the beam are shown in Figure 1, and its mounting with respect to the nozzle is shown in Picture 14. The strain gauge is mounted on the beam at the section s-s. The beam is in equilibrium in the position shown in Figure 2 (a). The bending moment at s-s caused by the force in the spray F is:

$$B = F_1 \ell + F_2 c \qquad (1)$$

$$B = F \times \ell \times \cos\theta + F \times c \times \sin\theta \qquad (2)$$

The strain S at the section s-s caused by the bending moment B is:

$$S = \frac{Bh}{2EI} \qquad (3)$$

Where:

E = Young's Modulus for phosphor bronze in pounds per square inch (psi)

I = Moment of inertia at the section s-s

h = Thickness of the phosphor bronze sheet in inches

The value of E can be found in any handbook, and is 16×10^6 psi

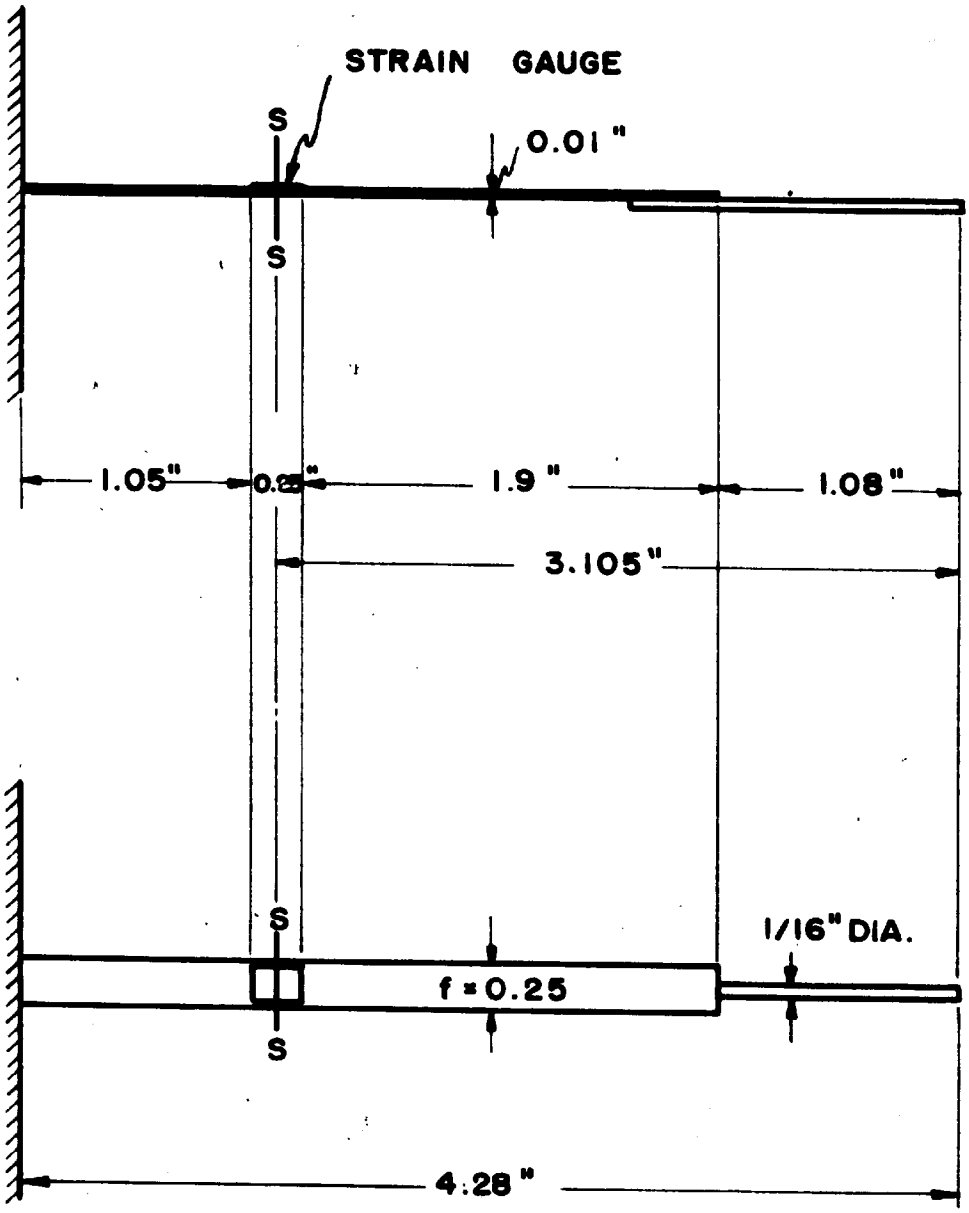

FIGURE 1

DIMENSIONS OF CANTILEVERED BEAM

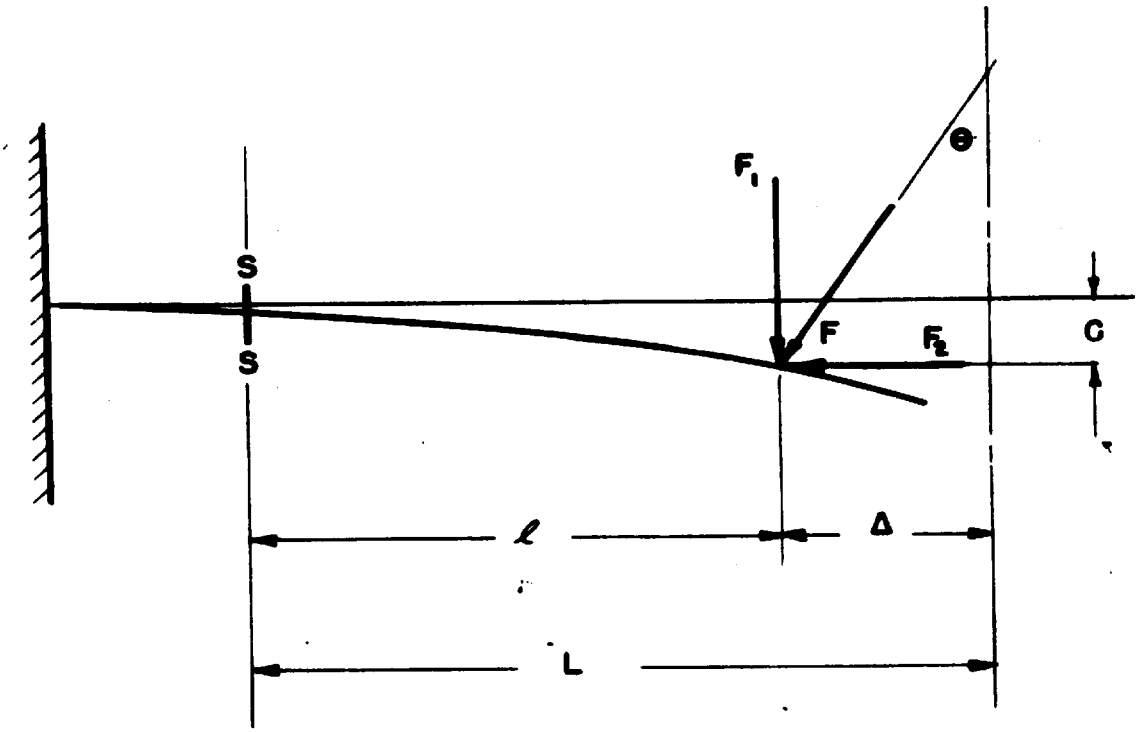

(a)

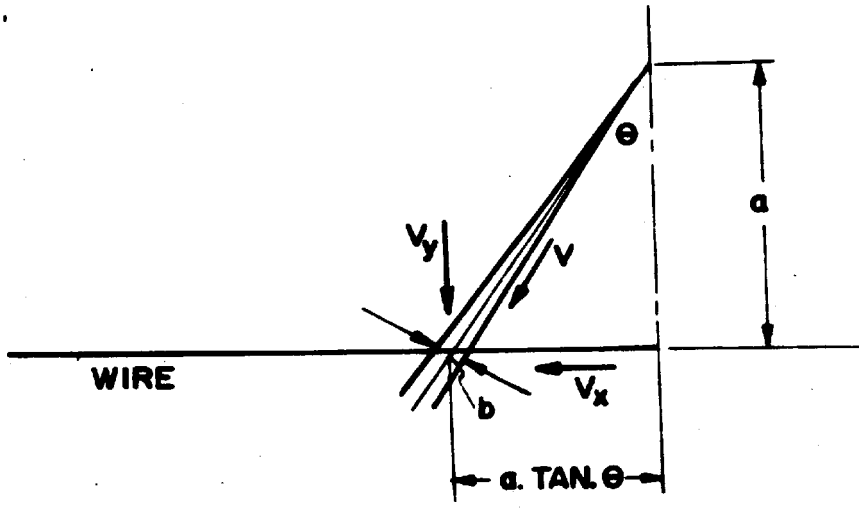

(b)

FIGURE 2

$I = \frac{fh^3}{12}$

f = width of phosphor bronze sheet in inches

The strain S is measured by the use of the strain gauge. Substituting for S,E,I and h in Equation 3, the bending moment B can be calculated.

By measuring half the spray angle θ, the deflection c, and the distance ℓ, the value of the mechanical force in the spray F can be calculated from Equation 2.

The second step after knowing the force in the spray is to find the thickness of the conical sheath of the spray as it leaves the nozzle.

The following calculations for the sheath thickness are based on the assumption that the flow of the fuel from the nozzle is in the form of a uniform and continuous conical sheath. It is also assumed that the wire is perfectly smooth so that there will be no force of friction between the wire and the fluid.

Let:

Q = Rate of flow of fluid through the nozzle in cubic feet per second

v = Velocity of the sheath in feet per second

v_y = Vertical component of velocity in feet per second

a = Height of nozzle above wire in feet

b = Thickness of the sheath at the point where it hits the wire in feet

g = Gravitational acceleration in feet per second per second

w = Specific weight of fuel used in pounds per cubic feet

M = Mass flow of fuel from the nozzle in pounds per second

Θ = Half the spray angle in degrees

F_y = The component of the mechanical force in the spray perpendicular to the wire (undeflected position) in pounds

A = Cross sectional area of the conical sheath at a distance "a" under the nozzle in square feet.

Hence:

$$V = \frac{Q}{A}$$

$$V = \frac{Q}{2\pi a \tan\Theta \, b} \qquad (4)$$

$$V_y = V \cos\Theta$$

$$M = \frac{Q_w}{g} \text{ lbs/sec.}$$

Since the velocity in the vertical direction after the impact of the fluid with the wire is zero, then:

$$\frac{d}{dt}(Mv_y) = Mv_y$$

$$F_y = Mv_y$$

$$= \frac{Q_w v_y}{g}$$

$$= \frac{Q_w v \cos\Theta}{g}$$

$$= \frac{Q_w Q \cos\Theta}{g 2\pi a \tan\Theta \, b}$$

$$F = \frac{F_y}{\cos\Theta}$$

$$= \frac{Q^2 w}{2\pi a \tan\Theta \, bg}$$

Hence:

$$b = \frac{Q^2 w}{2\pi a \tan\Theta \, Fg} \text{ feet} \qquad (5)$$

Apparatus:

The strain gauge Has the following characteristics:

Type	A_7
Gauge Factor	1.96
Resistance	120 ohms

This particular type was chosen as its overall dimensions suited the dimensions of the beam used.

The strain is measured by an SR-4 Baldwin Strain Indicator, Number D43253. This is an a-c bridge circuit with the active strain gauge as an arm. The bridge measures the change in the resistance of the active strain gauge caused by its extension or contraction. The block diagram of the SR4 strain indicator is shown in Figure 3 and the detailed circuit diagram is shown in Figure 4.

To compensate for any heat effects on the strain gauge wire, a so-called compensating gauge is used. This is the same type of gauge as the one used to measure the strain and it is mounted on a similar piece of phosphor bronze and placed in the chamber containing the spray. It forms another arm of the a-c bridge circuit.

The beam is mounted on a vertical hollow shaft placed axially under the nozzle. The shaft can be rotated at a speed of about 1 r.p.m. by the use of an electric motor and a reduction gear placed under the spray chamber. The distance between the beam and the nozzle can be adjusted by moving the shaft upwards or downwards. The tip of the wire must be vertically under the tip of the nozzle for complete symmetry.

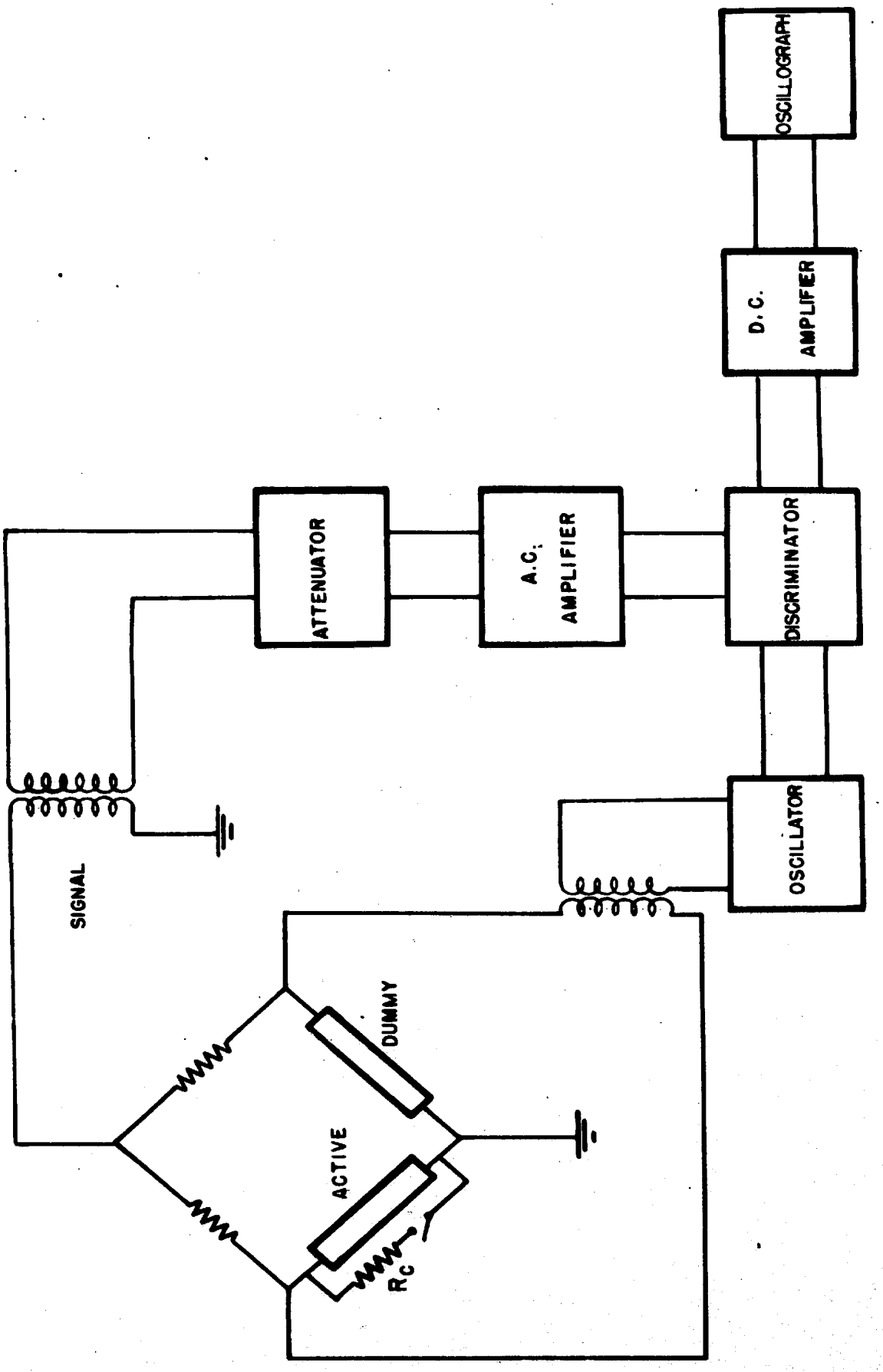

FIGURE 3

BLOCK DIAGRAM OF STRAIN ANALYZER

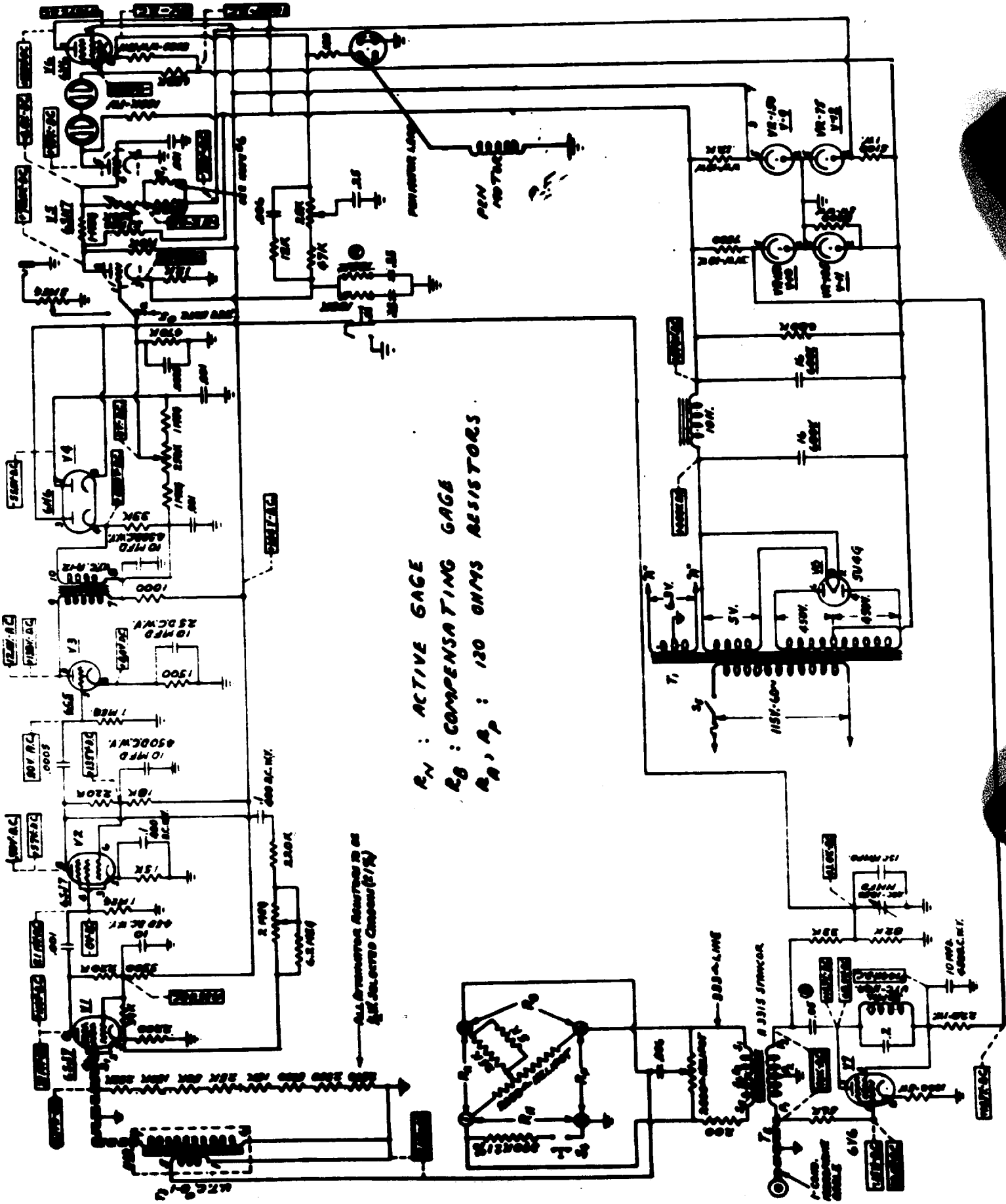

FIGURE 4

CIRCUIT DIAGRAM OF STRAIN ANALYZER

The two leads from the active gauge are led through the hollow vertical shaft, each dipping into mercury in a shallow plexiglass container mounted co-axially with the shaft under the spray chamber as shown in Figure 5. This arrangement served as slip rings. The use of ordinary copper or carbon slip rings was not possible because the change in the resistance of such slip rings is much larger than the order of sensitivity of the gauge.

To be able to record the readings of the strain as the beam is rotated around in the spray, a Type BL 202, Number 1255 Brush oscillograph is used. The circuit diagram of the oscillograph is shown in Figure 6. It is connected as shown in Figure 4, to the meter terminals of the SR4 strain indicator through a Type BL 913, Number 884, Brush d-c amplifier. The use of the d-c amplifier is necessary because the signal through the SR4 meter is very small since it is the difference between the rectified signal voltage and the rectified oscillator voltage of the a-c bridge.

A cam geared to the rotating shaft and rotating at 1/2 the shaft speed activates a micro-switch which starts and stops the recording oscillograph. The oscillograph records during 1/2 the cycle of the cam, i.e., one cycle of the shaft, and stops recording during the other half cycle. This is necessary to produce records corresponding exactly to three hundred and sixty degrees of rotation which facilitates comparison between records of different nozzles.

The vertical deflection c of the beam caused by the force of the spray, the spray angle θ, and the point where the

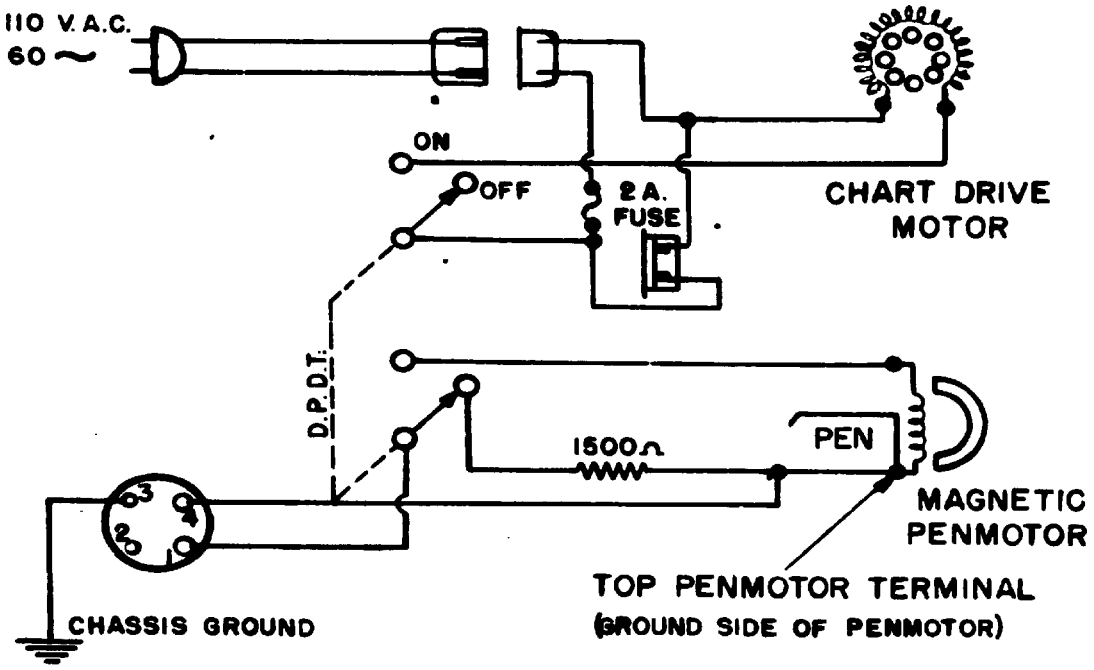

FIGURE 6

BRUSH OSCILLOGRAPH BL-201 CIRCUIT DIAGRAM

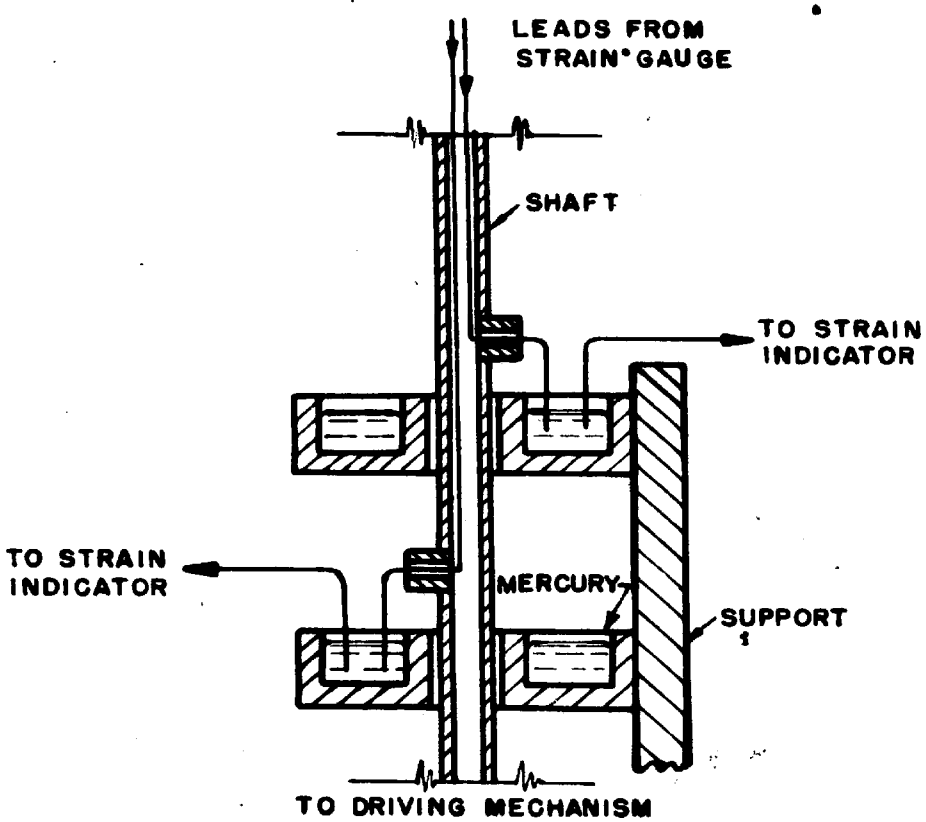

FIGURE 5

MERCURY BATH SET-UP

spray hits the beam remain to be measured. This is carried out by mounting a plexiglass sheet, divided into 0.1 inch side squares, on one side of the cubic glass chamber containing the spray. A telescope set at the same level as the beam is used to locate the point of intersection of the wire and the spray on the plexiglass sheet. It also serves the purpose of measuring half the spray angles. A strong spotlight is used to illuminate the conical sheath as it leaves the nozzle to make it easier to locate the point of intersection of the sheath and the wire. At high pressures, it is almost impossible to see the wire or the nozzle through the telescope because of the fog created by the small drops hanging in the chamber.

The nozzles used in this test are mostly of the simplex type, although the test can be run on single or double port duplex nozzles as well. The fuel (kerosene) is pumped through the nozzle by a low pressure and a high pressure pump. Different pressure gauges and flow-rate meters are placed on the panel board for measuring the pressure and the rate of flow of the liquid through the nozzle. The panel board and the piping system are shown in Pictures 16 and 17, respectively.

Pictures 9 and 10 show a somewhat similar apparatus in which a slender cupro-nickel wire was inserted in the spray sheath. The wire was elongated because of the impulse of the spray and the resulting change in the wire resistance was measured by a bridge circuit. However, it was found difficult to maintain uniform tension in the wire because of the instability of the supports. In addition, vibrations were produced in the supports of the wire causing strains on it as great as

those caused by the spray itself. Thus, further experimentation with the slender wire was discontinued at that time, and the apparatus described above was devised instead.

Results:

The results obtained from this experiment serve two different purposes. First of all, the absolute value of the sheath thickness of the fuel spray in the direct vicinity of the nozzle was obtained in the following manner. With the beam placed 0.55 inches under the nozzle and stationary at a particular point, the fuel pressure was varied from 50 to 500 psi and readings were obtained for every 50 psi interval. From this data, the sheath thickness corresponding to each fuel pressure can be calculated, and the variation of the sheath thickness with pressure can be studied. This test was performed on nozzle Number 6702074 A -2/3 DED C52 three different times and the resulting data is included in Tables 1, 2, and 3.

In addition, this experiment served still another purpose. This was the study of the thickness of the fuel sheath around its entire circumference, which reveals any imperfections in the outlet of the nozzle. The beam was rotated at 1 r.p.m. in the spray, and an oscillograph chart was obtained for each fuel pressure. Any variations of the fuel sheath thickness would hence be revealed by an examination of these charts. Figures 7, 8, and 9 show the charts for a good nozzle at different fuel pressures, while Figures 10, 11, and 12 show the charts for an intentionally defaced nozzle.

TABLE 1

DATA ON SPRAY OF NOZZLE 6702074 A - 2/3 DED C52

(STRAIN GAUGE)

a = 0.55 in.

No.	Press. in #/sq.in	Discharge in #/hour	SR 4 Readings Zero	Final	Strain	θ	Vert. Def. c	Hor. Dist. From end	Force in Grams	Sheath. Thick. b
1	50	62	550	554	4	32°30'	0.00	0.35	0.0525	0.107
2	100	160	550	572	22	36 --	0.00	0.40	0.300	0.108
3	150	213	553	610	57	34 40	0.10	0.45	0.805	0.075
4	200	250	532	622	90	32 35	0.15	0.45	1.175	0.077
5	250	290	550	658	108	35 30	0.15	0.50	1.480	0.072
6	300	328	560	690	130	35 10	0.20	0.55	1.775	0.076
7	350	360	570	720	150	35 10	0.20	0.55	2.050	0.079
8	400	390	580	750	170	34 30	0.25	0.55	2.280	0.090
9	450	414	580	780	200	34 30	0.25	0.55	2.690	0.086
10	500	445	600	820	220	-- --	--	--	--	--



TABLE 2

DATA ON SPRAY OF NOZZLE 6702074 A - 2/3 DED C52

(STRAIN GAUGE)

a = 0.55 in.

No.	Press. in #/sq.in	Discharge in #/hour	SR 4 Readings Zero	Final	Strain	θ	Vert. Def. c	Hor. Dist. From end	Force in Grams	Sheath Thick. b
1	50	70	567	571	4	36°--	0.00	0.40	0.055	0.113
2	100	151	562	582	20	33 40	0.05	0.40	0.264	0.120
3	150	207	570	620	50	34 40	0.10	0.45	0.670	0.087
4	200	242	570	660	90	38 --	0.15	0.55	1.300	0.053
5	250	288	570	675	105	38 --	0.15	0.55	1.520	0.052
6	300	330	575	710	135	38 --	0.20	0.55	1.940	0.066
7	350	360	570	720	150	38 36	0.20	0.60	2.165	0.069
8	400	392	590	760	170	40 40	0.25	0.65	2.490	0.066
9	450	420	580	780	200	40 50	0.25	0.65	2.980	0.063
10	500	445	600	830	230	-- --	--	--	--	--



TABLE 3

DATA ON SPRAY OF NOZZLE 6702074 A - 2/3 DED C52

(STRAIN GAUGE)

a = 0.55 in.

No.	Press. in #/sq.in.	Discharge in #/hour	SR 4 Readings Zero	Final	Strain	θ	Vert. Def. c	Hor. Dist. From end	Force in Grams	Sheath Thick. b
1	50	66	749	754	5	32°--'	0.000	0.25	0.060	0.098
2	100	160	749	771	22	34 40	0.050	0.40	0.284	0.074
3	150	211	746	802	56	34 30	0.075	0.45	0.736	0.074
4	200	245	752	822	70	34 30	0.150	0.45	0.900	0.082
5	250	290	751	859	108	39 20	0.180	0.47	1.570	0.055
6	300	325	742	873	131	38 40	0.200	0.60	1.850	0.060
7	350	345	719	880	161	38 --	0.200	0.50	2.160	0.060
8	400	386	712	908	196	-- --	--	--	--	--



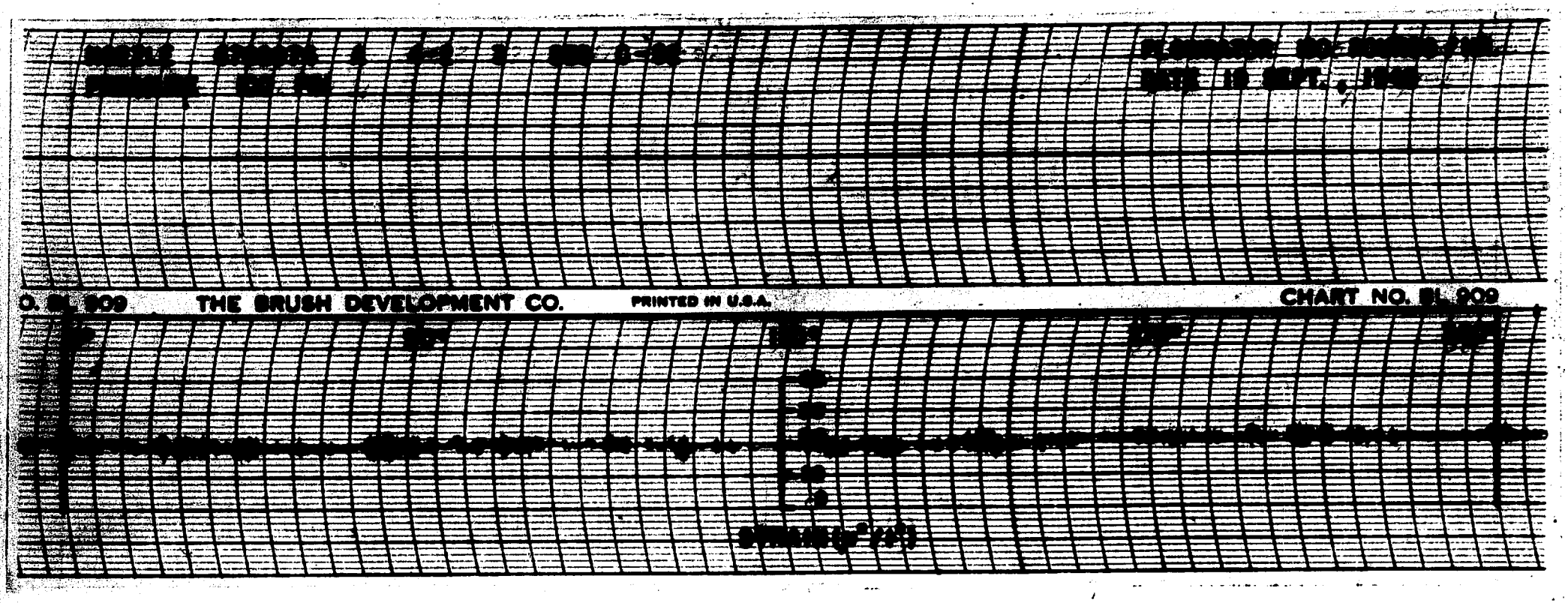

FIGURE 7

OSCILLOGRAPH CHART FOR SIMPLEX NOZZLE 6702074 A 4-2/3 DED C52

(STRAIN GAUGE)

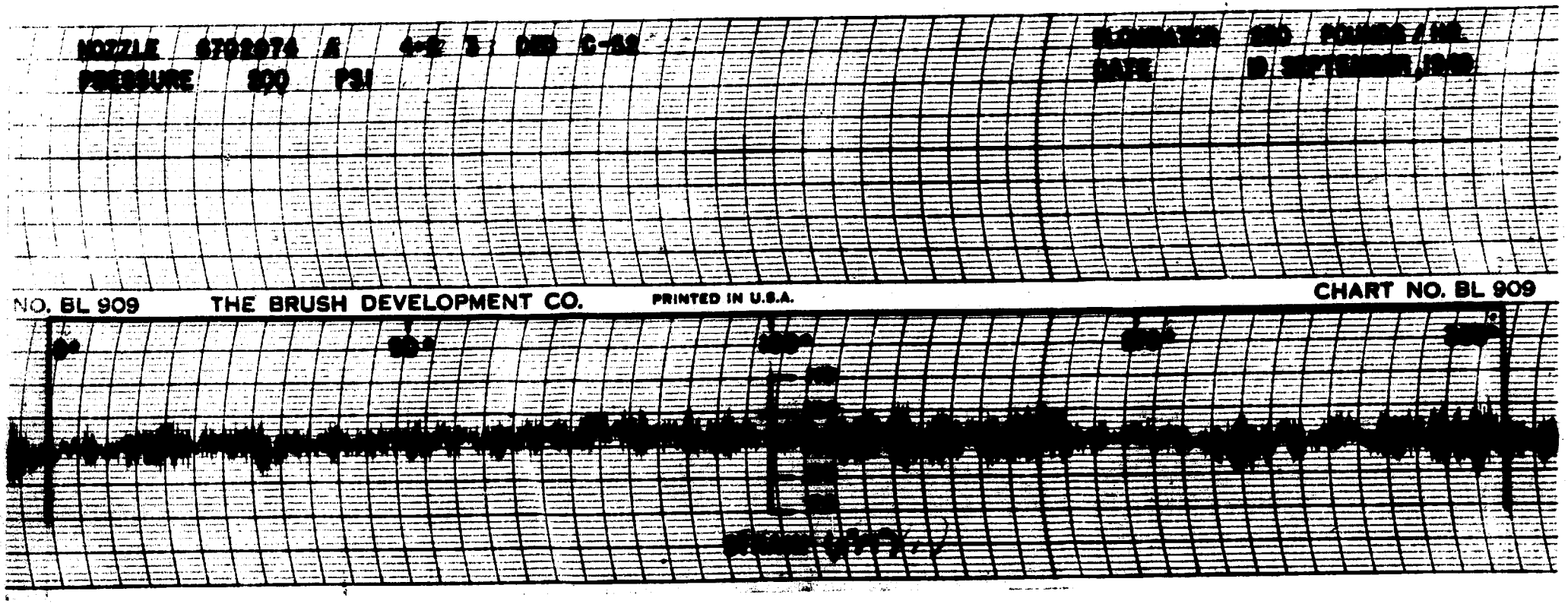

FIGURE 8

OSCILLOGRAPH CHART FOR SIMPLEX NOZZLE 6702074 A 4-2/3 DED C52

(STRAIN GAUGE)

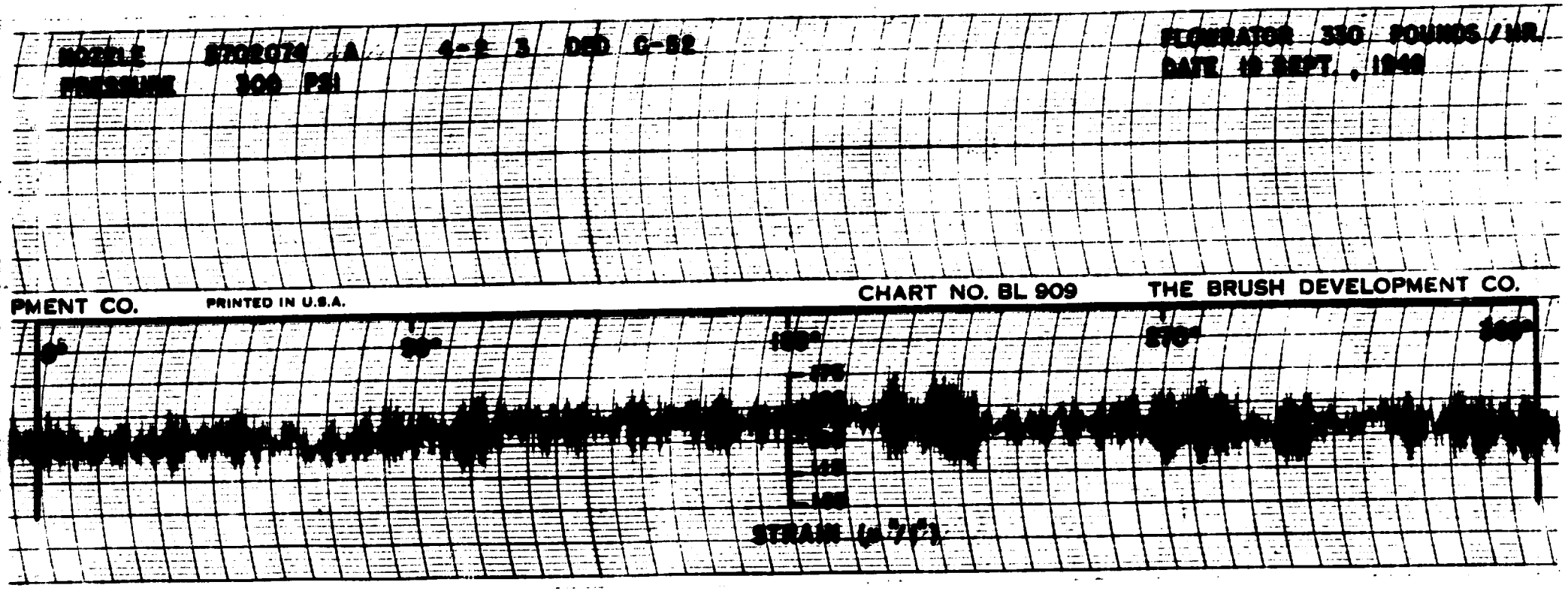

FIGURE 9

OSCILLOGRAPH CHART FOR SIMPLEX NOZZLE 6702074 A 4-2/3 DED C52

(STRAIN GAUGE)

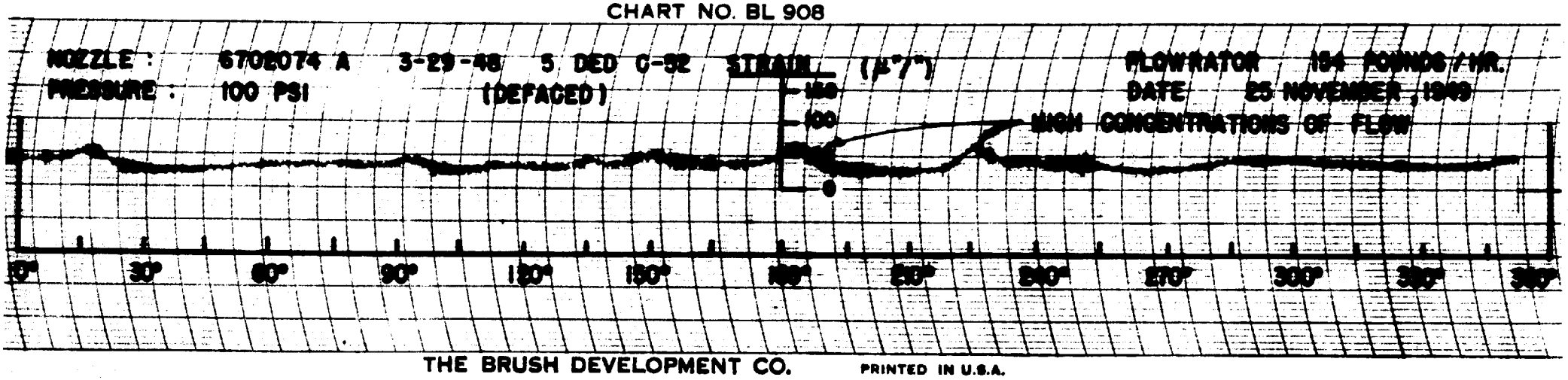

FIGURE 10

OSCILLOGRAPH CHART FOR DEFACED SIMPLEX NOZZLE 6702074 A 3-29-48 5 DED C52

(STRAIN GAUGE)

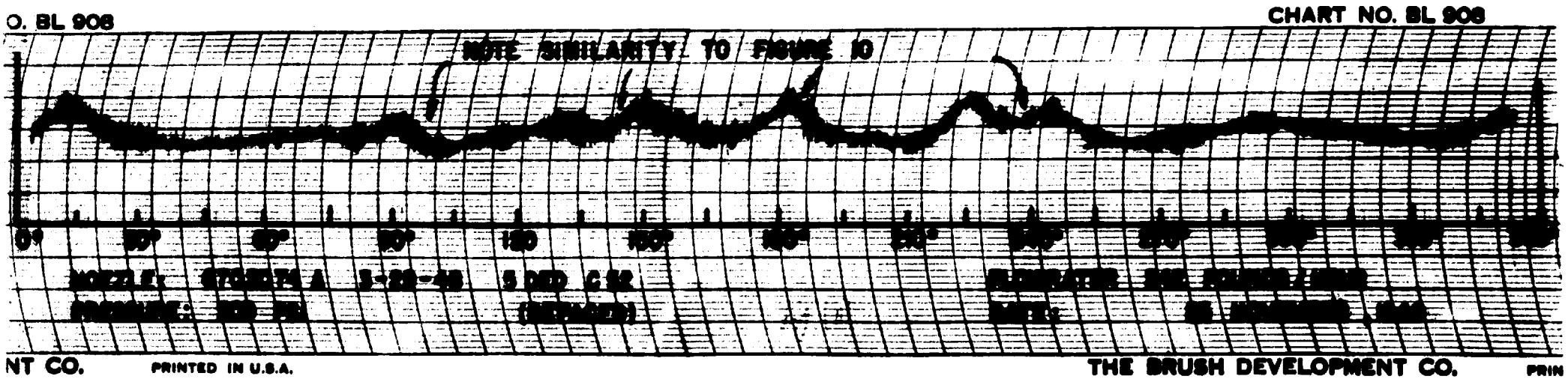

FIGURE 11

OSCILLOGRAPH CHART FOR DEFACED SIMPLEX NOZZLE 6702074 A 3-29-48 5 DED C52

(STRAIN GAUGE)



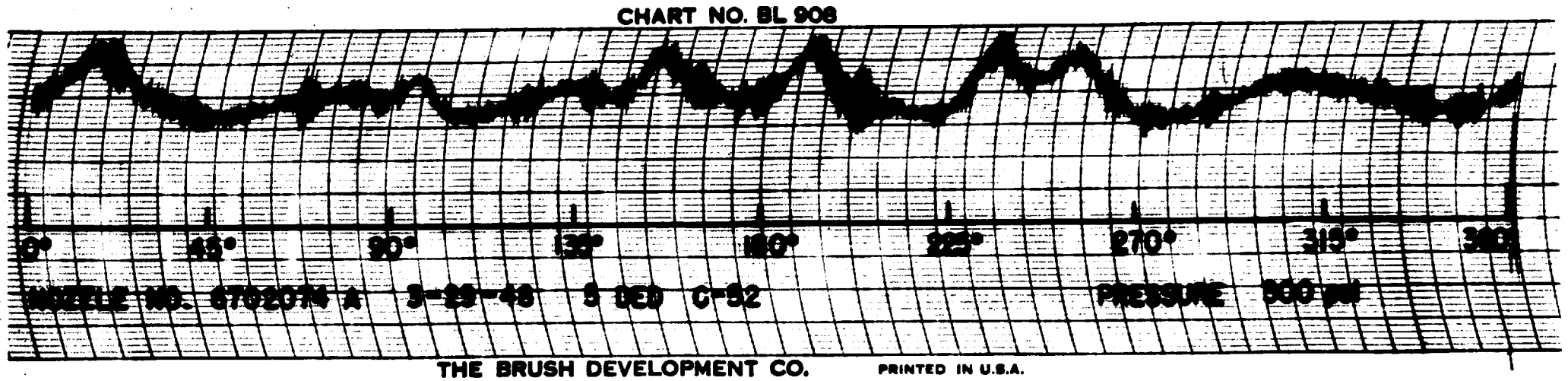

FIGURE 12

OSCILLOGRAPH CHART FOR DEFACED SIMPLEX NOZZLE 6702074 A 3-29-48 5 DED C52

(STRAIN GAUGE)

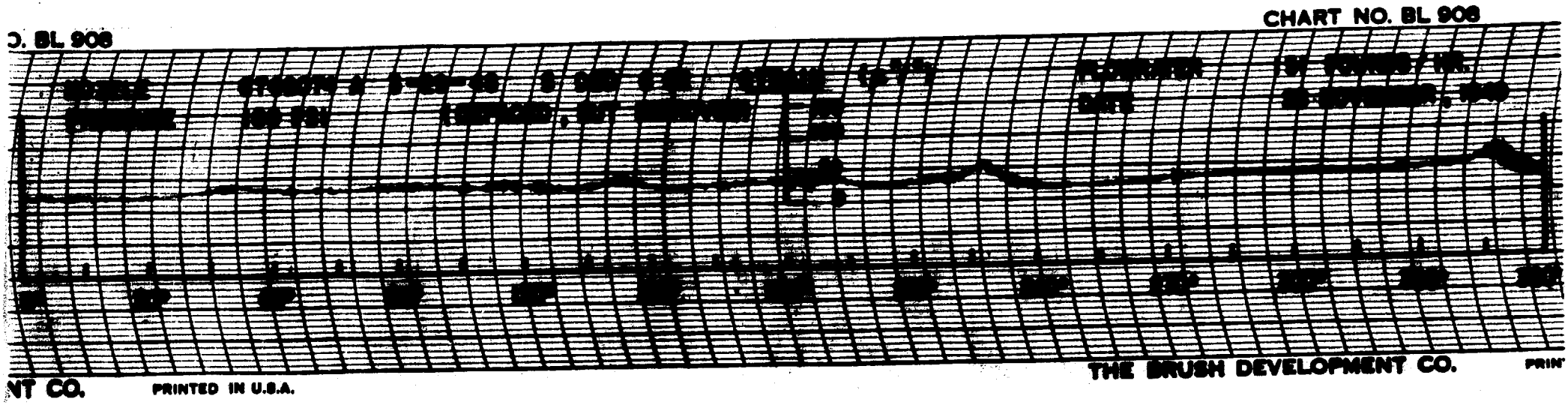

FIGURE 13

OSCILLOGRAPH CHART FOR DEFACED (BUT IMPROVED) SIMPLEX NOZZLE 6702074 A 3-29-48 5 DED C52

(STRAIN GAUGE)

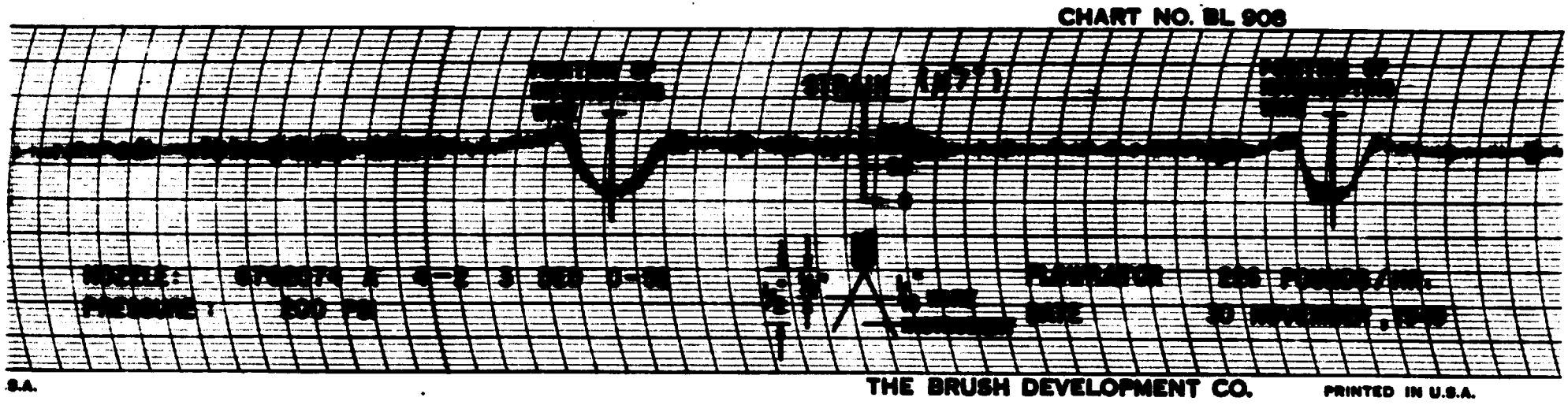

FIGURE 14

OSCILLOGRAPH CHART FOR SIMPLEX NOZZLE 6702074 A 4-2/3 DED C52
WITH 1/16" WIRE INSERTED IN THE SPRAY

(STRAIN GAUGE)

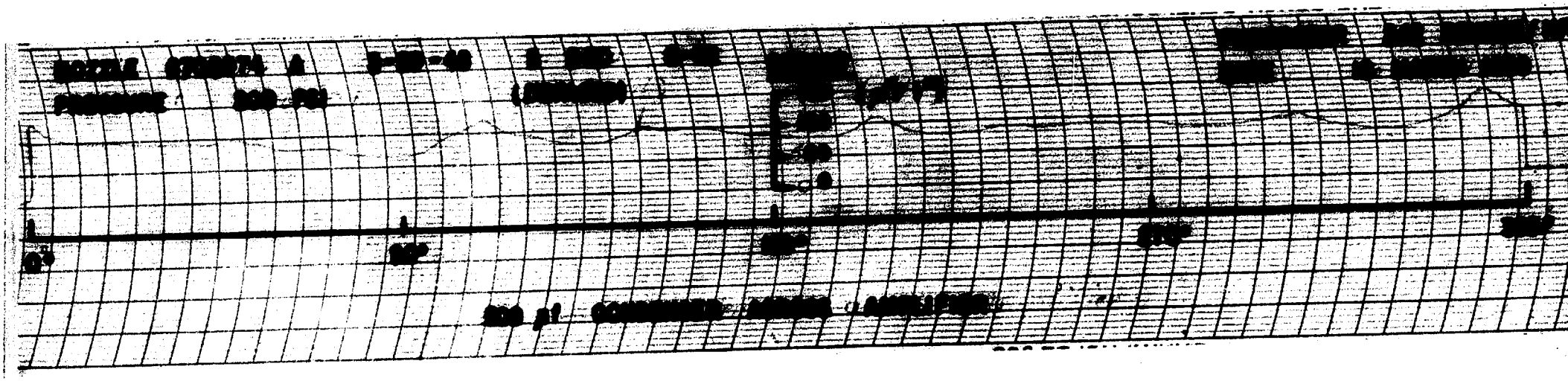

FIGURE 15

OSCILLOGRAPH CHART FOR DEFACED SIMPLEX NOZZLE 6702074 A 3-29-48 5 DED C52
USING A 500 u.f. CONDENSER ACROSS AMPLIFIER

(STRAIN GAUGE)

Only simplex nozzles were tested in this experiment, but any other type of nozzle (single or double port duplex) could be substituted.

Discussion of Results:

The charts in Figures 7, 8, 9, 10, 11, and 12 show that instead of uniform lines, the oscillograph records parasitic vibrations of the beam caused by the excitation of its natural frequency (13 cycles per second) by the vibrations of the fuel pumps. To reduce the amplitude of these vibrations, the beam was made heavier by substituting a thicker piece of phosphor bronze. This proved unsatisfactory since the sensitivity of the instrument was reduced.

By studying the charts taken for the nozzle Number 6702074 A - 2/3 DED C52, it is found that the change in the recorded force along the circumference is small for all the different pressures between 50 and 500. This shows that the thickness of the sheath produced by this nozzle is uniform, which leads to the conclusion that the spray of this nozzle is uniform and would not produce hot spots in the combustion chamber of the aircraft engine.

Examining the charts for the defaced nozzle Number 6702074A 3-29-48-5 DED C-52 and comparing it with the microphotograph of the nozzle tip shown in Picture 11, it appears that the notches in the nozzle have little or no effect in producing non-uniformity in the sheath, whereas the burrs contribute most of the non-uniformity. This may be the reason why the nozzles cannot be used satisfactorily more than 100 hours in actual service

because of the carbon deposits at the tip of the nozzle. The value of the thickness of the sheath for nozzle Number 6702074 A - 2/3 DED C52 is calculated from the data included in Tables 1, 2, and 3 as demonstrated in Appendix I. It is found that, for a fixed distance between the nozzle and the probe, the sheath thickness varies with the pressure of the fuel supplied to the nozzle. It goes down with increase in pressure reaching a minimum then rising again, as shown in Figure 16. It is believed that after this critical pressure, in this case 250 pounds per square inch for the particular distance between probe and nozzle, the sheath starts to disintegrate into small drops before hitting the probe. The value of the thickness of the sheath is then that of a solid sheath that would produce the same force on the probe as the drops.

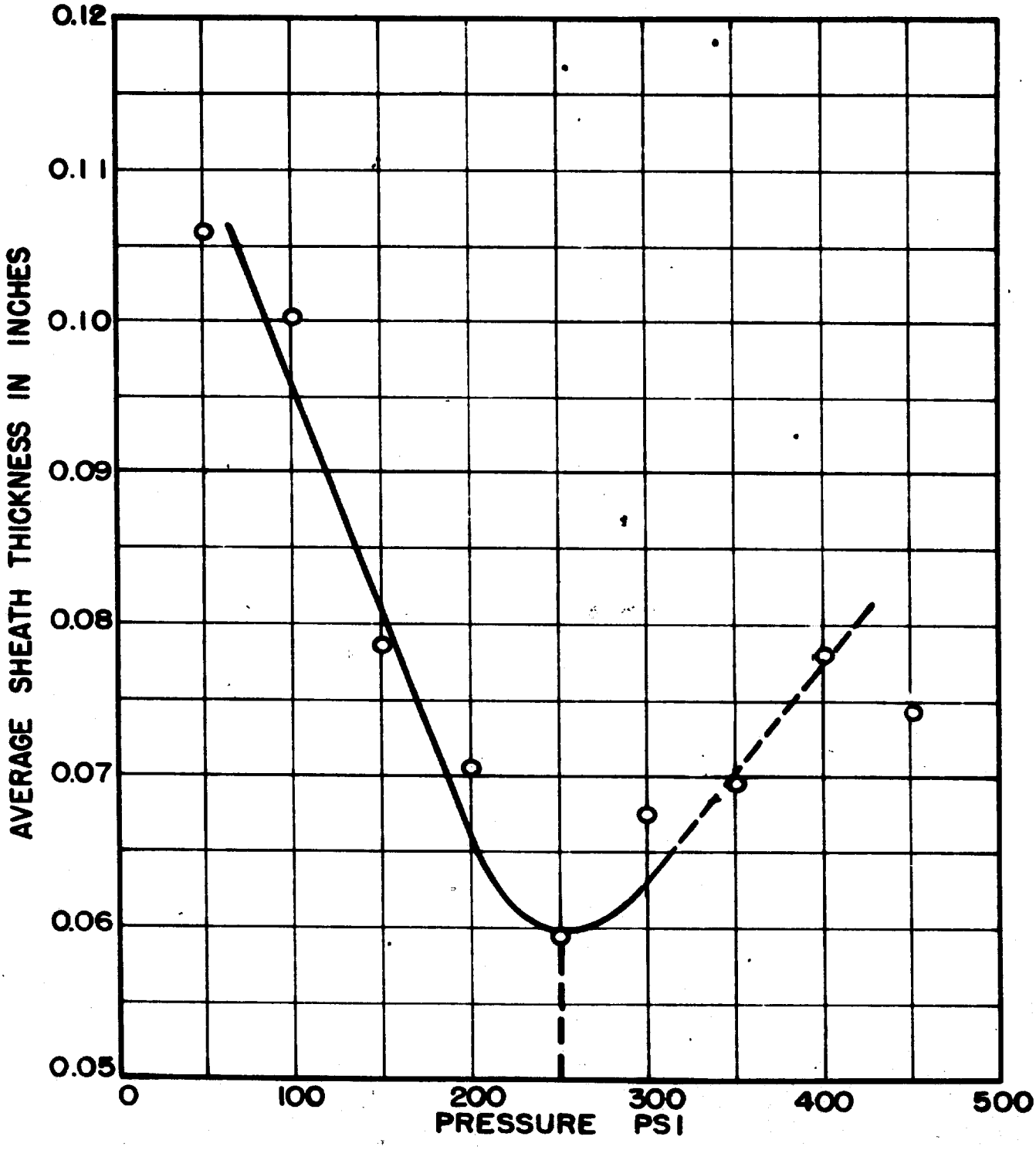

FIGURE 16
VARIATION OF SHEATH THICKNESS WITH PRESSURE FOR SIMPLEX NOZZLE 6702074 A 4-2/3 DED C 52

CHAPTER II

TUBE ANALYZER

Theory:

This method is essentially the same as the first method but a different pick up is used. The sheath thickness is determined by measuring the force of the spray. The RCA 5734 vacuum tube, called the mechano-electronic transducer, serves as the pick up.

The main features of the tube are shown in Figure 17 and its operation can be briefly explained as follows. The motion of the movable anode E in the direction M-M is transfered through the thin metal diaphragm D to produce a proportional change in the electron flow of the triode formed by cathode K, grid G, and plate E. The envelope S is metallic and serves as the plate lead. The diaphragm D is very thin and acts as a flexible window in the tube envelope. Through this vacuum tight metal diaphragm the rod, used as a lever, is free to vibrate without distortion over a wide range of frequencies. The tube is sensitive only in one plane of motion of the anode E. The complete details of the characteristics and the operation of the tube can be found in the RCA tube manual listed under Number 5734.

A few modifications are necessary to make the tube suitable for the study of sheath thickness. A piece of thin, hollow nickel tubing is fitted snugly onto the plate shaft for use as the probe to be introduced in the spray. Since the tube is designed primarily as a vibration pick up its diaphragm D

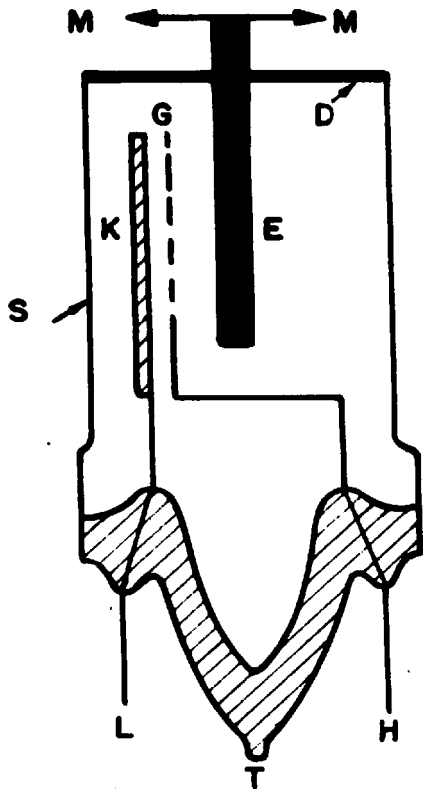

FIGURE 17
SCHEMATIC DIAGRAM OF THE RCA 5734
MECHANO-ELECTRONIC TRANSDUCER

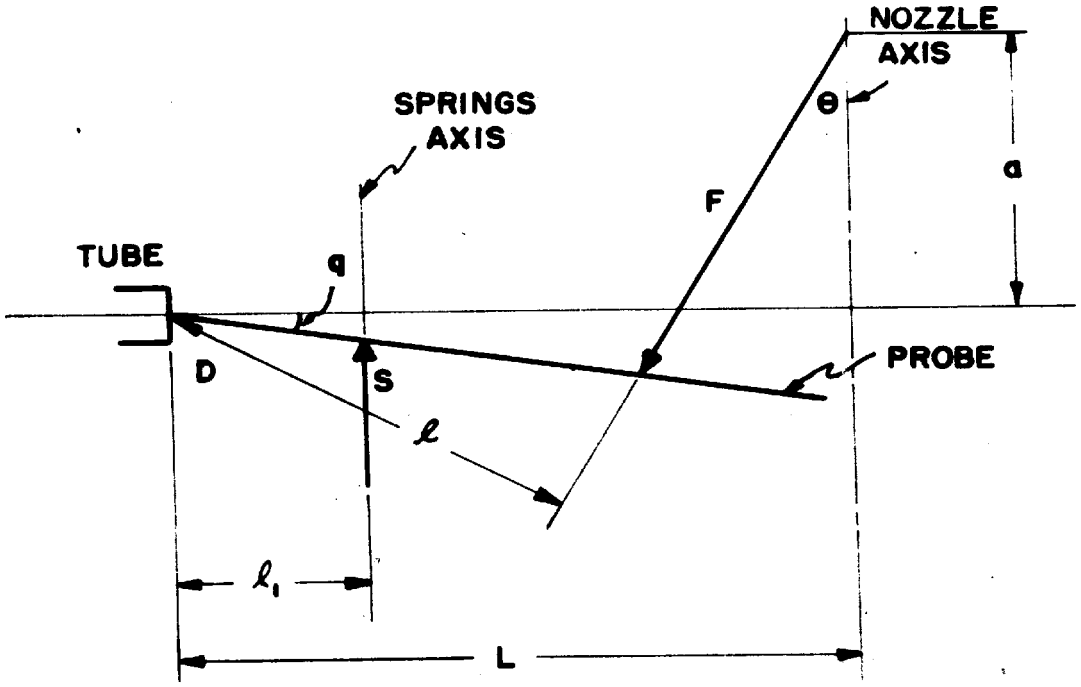

FIGURE 18
POSITION OF EQUILIBRIUM OF TUBE ARM

supplies no restoring force at the plate shaft. An external restoring force is supplied by the use of two light springs so that it can be used for static measurements with the plate shaft floating. The springs are attached one on each side of the nickel tubing as shown in Picture 18.

The following analysis shows the relation between the torque produced by the spray force and the angular deflection of the pick up arm, assuming the diaphragm D does not restore any moment.

Let:

k = spring constant

F = spray force

Θ = half spray angle

S = force produced by the springs

q = angular deflection of the arm caused by the force F

T = torque of the spray force at the diaphragm D

ℓ = force arm

a = vertical distance between nozzle and tube axis before the spray starts

The tube arm is in equilibrium in the position shown in Figure 18.

As q lies between plus and minus 0.5 degrees according to the tube specifications, it is justified to assume that

$q = \tan q$

$\ell = (L - a \tan\Theta) \cos\Theta$ (6)

Assuming the two springs to be exactly identical

$S = 2k\ell_1 \tan q$

$S = 2k\ell_1 q$

Taking moments around D we get:

$S\ell_1 = F\ell = T$

$T = 2k\ell_1^2 q$

But k and ℓ_1 are constants, hence

$q = \text{constant} \times T$

Thus the applied torque is proportional to the angular deflection of the shaft. Hence T is proportional to the voltage across the load on the tube.

The tube is calibrated by applying known torques to its diaphragm and measuring the change in the output voltage across its resistive load. These calibration curves are taken for different distances between the position of the springs and the diaphragm until the best position is found. This position gives the highest sensitivity without destroying the tube.

In actual use, the output voltage of the tube corresponding to a given spray is measured and its corresponding torque found from the calibration charts. Then by measuring half the spray angle Θ, and the point of intersection of the spray and the probe, the force arm can be calculated from Equation (6) and hence the force of the spray can be found.

The sheath thickness b is found by the application of Equation (5) of the first method, namely:

$$b = \frac{Q^2 w}{2\pi a \tan\Theta \, Fg} \quad \text{feet}$$

Apparatus:

The tube is mounted as shown in Picture 18 with the tip of the nickel tubing probe placed directly under the nozzle. The leads from the tube are run within the hollow vertical shaft, which carries the bracket on which the tube is mounted, to slip rings placed under the spray chamber. The same driving mechanism mentioned in the first experiment is again used here to rotate the vertical shaft. The cam and microswitch arrangements are also used again to get records corresponding to exactly three hundred and sixty degrees of rotation.

The electrical circuit diagram for the tube analyzer is shown in Figure 19. Two RCA 5734 tubes, together with their load resistances R_1 and R_2, are used to form a bridge circuit. The use of this type of circuit is necessary to buck out the change in voltage across the resistive load of the active tube, Number (1), caused by the applied torque. The resistances R_1 and R_2 are wire wound precision resistances which are not affected by variations in temperature. Dry batteries are used as the d-c power supply for the plate and filament voltages of the tubes to avoid 60 cycle pick up which would result from using a regular power supply. The d-c amplifier used is the Type B.L. 913 Brush Number 884 with a full gain of 2000 which was also used in the first method. It serves as a matching impedance between the bridge circuit and the recording oscillograph. Its circuit diagram is shown in Figure 20. The oscillograph used is the single channel Type B.L. 202 Brush Number 1255 with variable chart speeds.

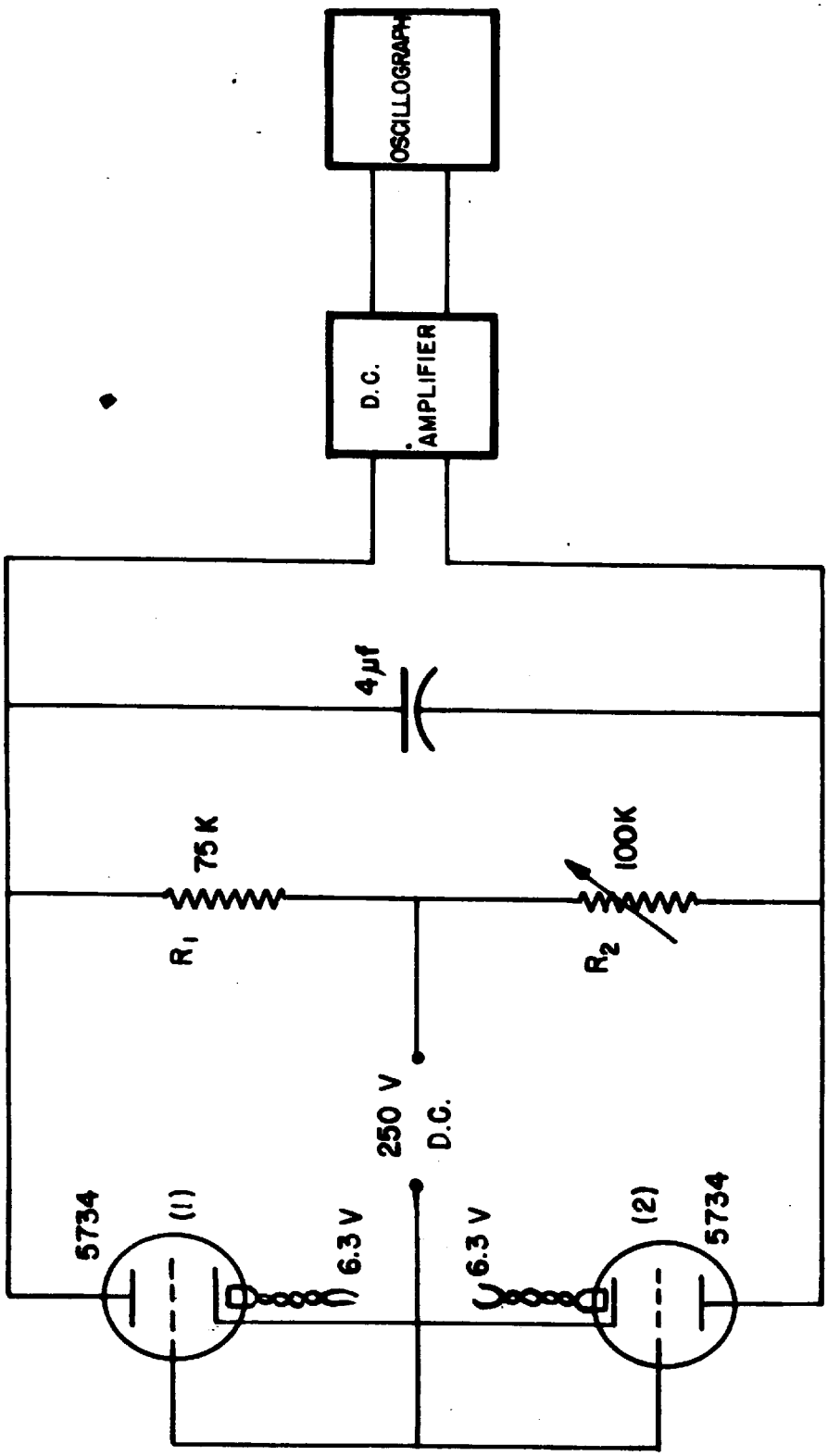

FIGURE 19
CONNECTION DIAGRAM FOR TUBE ANALYZER

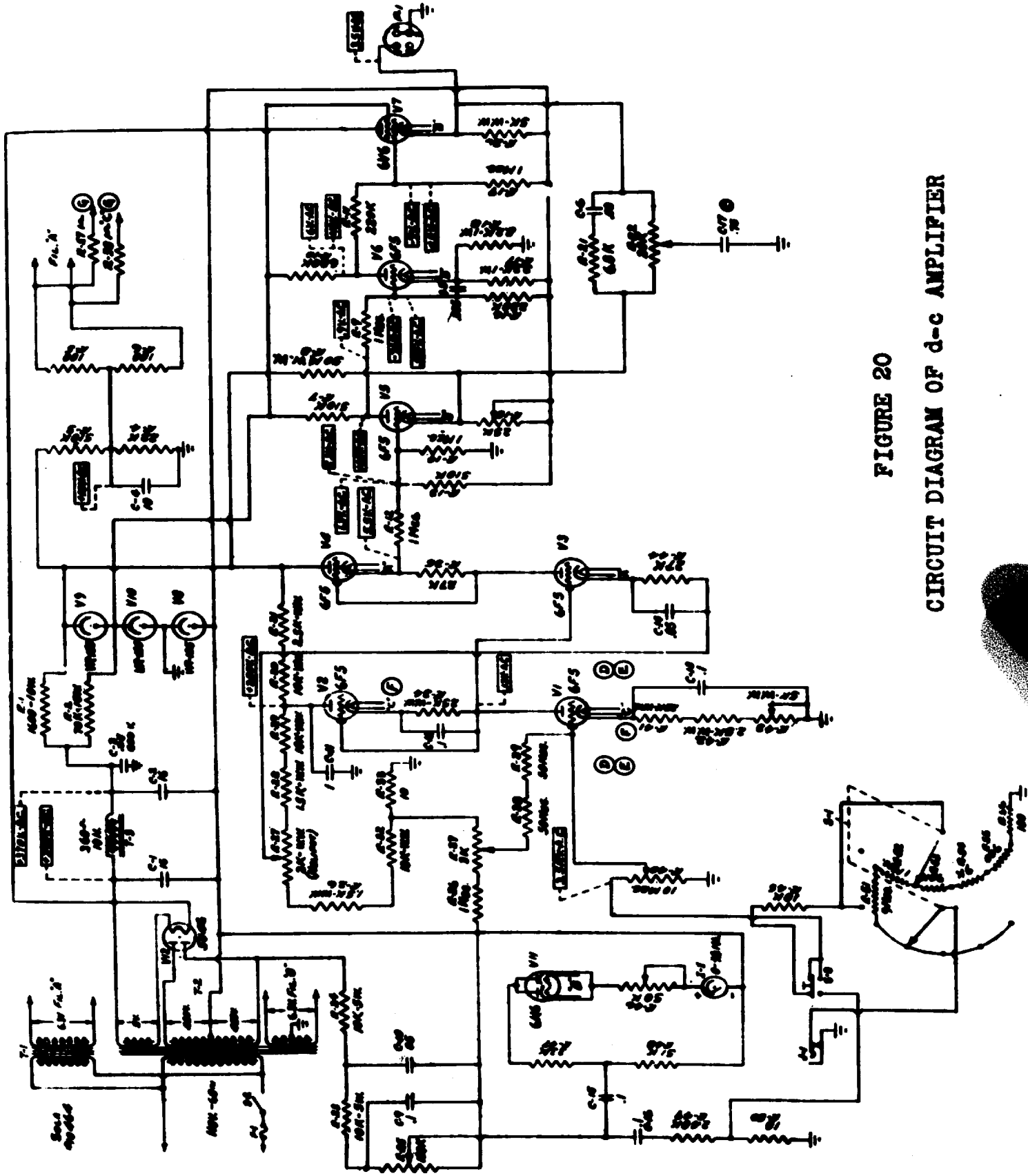

FIGURE 20

CIRCUIT DIAGRAM OF d-c AMPLIFIER

With the tube analyzer connected as described above, the oscillograph records parasitic vibrations in the springs and the probe. The charts obtained are similar to those of the first method but the amplitude of the vibrations are more uniform. In order to minimize these vibrations so that clearer charts could be obtained, the springs were made heavier. This was not successful since it reduced the sensitivity of the instrument. Instead, a condenser of 4 microfarads was placed across the input terminals of the amplifier. This condenser acts as a by-pass to all the noise and vibration currents. The charts obtained thus are clearer as can be seen in Figures 27 and 28. The use of the condenser does not affect the main signal as the speed of rotation of the probe is only 1 r.p.m.

The use of two tubes as two arms of the bridge led to the idea of using them actively by mounting them so they would be deflected by the spray in oppposite directions, i.e., push-pull operation. The tubes were connected electrically as shown in Figure 19. Theoretically, this would make the instrument doubly sensitive, as discussed in Appendix III.

Picture 19 shows how the two tubes were mounted side by side in a plastic support. This support was mounted on the same rotating vertical shaft which was used with the single tube. The light springs were again used to provide a restoring force. Considerable mechanical difficulties were encountered in attaching the lever arm to both plate shafts.

The calibration tests of the double tube arrangement show only a slight increase in sensitivity over the use of one tube,

instead of the theoretical doubled sensitivity, as can be seen by comparison of Figures 21 and 22. This loss in sensitivity is caused by mechanical imperfections in the mounting of the two tubes. In reference to Picture 19, it can be seen that the tubes are contained in a plexiglass mounting which insulates them from each other. Two pieces of the hollow nickel tubing were fitted on the plate shafts M_1 and M_2, as shown in opposite Figure. The use of the plexiglass block A was necessary to insulate M_1 from M_2. This was a crude device for mounting the tubes which resulted in the reduced sensitivity of the double tube arrangement. However, if a proper mechanical mounting is devised, the use of the two tubes actively will give greater sensitivity. The tests included in this work were performed by using the single tube arrangement.

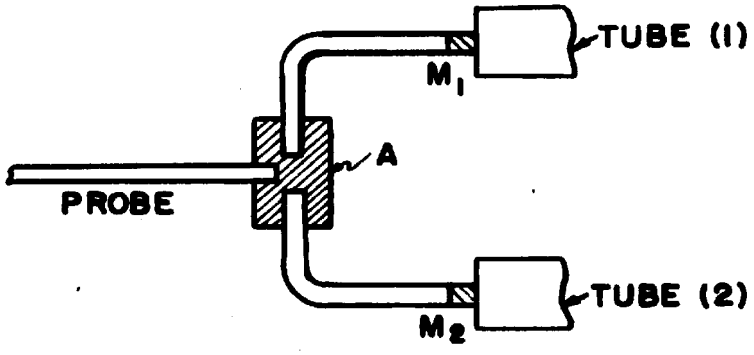

Results:

Tables 4 and 5 include the results of the calibration tests on the single and double tube arrangements. These tests were made by suspending known weights from the probe at a certain distance from the tube diaphragm and measuring the corresponding voltage change across the bridge terminals.

TABLE 4

CALIBRATION OF ONE TUBE

Distance between springs and tube diaphragm D = 1.5 cm

Force arm = 3 cm

Load gms	Torque gm.cms	Run 1 Voltage	Run 2 Voltage	Run 3 Voltage	Average Voltage
0.0	0.0	0.0	0.0	0.0	0.0
0.2	0.6	0.2	0.2	0.25	0.216
0.5	1.5	0.6	0.6	0.6	0.60
0.7	2.1	---	0.9	0.825	0.8625
1.0	3.0	1.3	1.3	1.32	1.306
1.2	3.6	1.65	1.55	1.58	1.593
1.5	4.5	1.95	1.96	1.975	1.9616
1.7	5.1	2.25	2.2	---	2.225
2.0	6.0	2.65	2.6	2.65	2.63
2.2	6.6	---	---	2.90	2.90
2.5	7.5	3.30	3.2	3.40	3.30
3.0	9.0	4.05	4.0	---	4.025

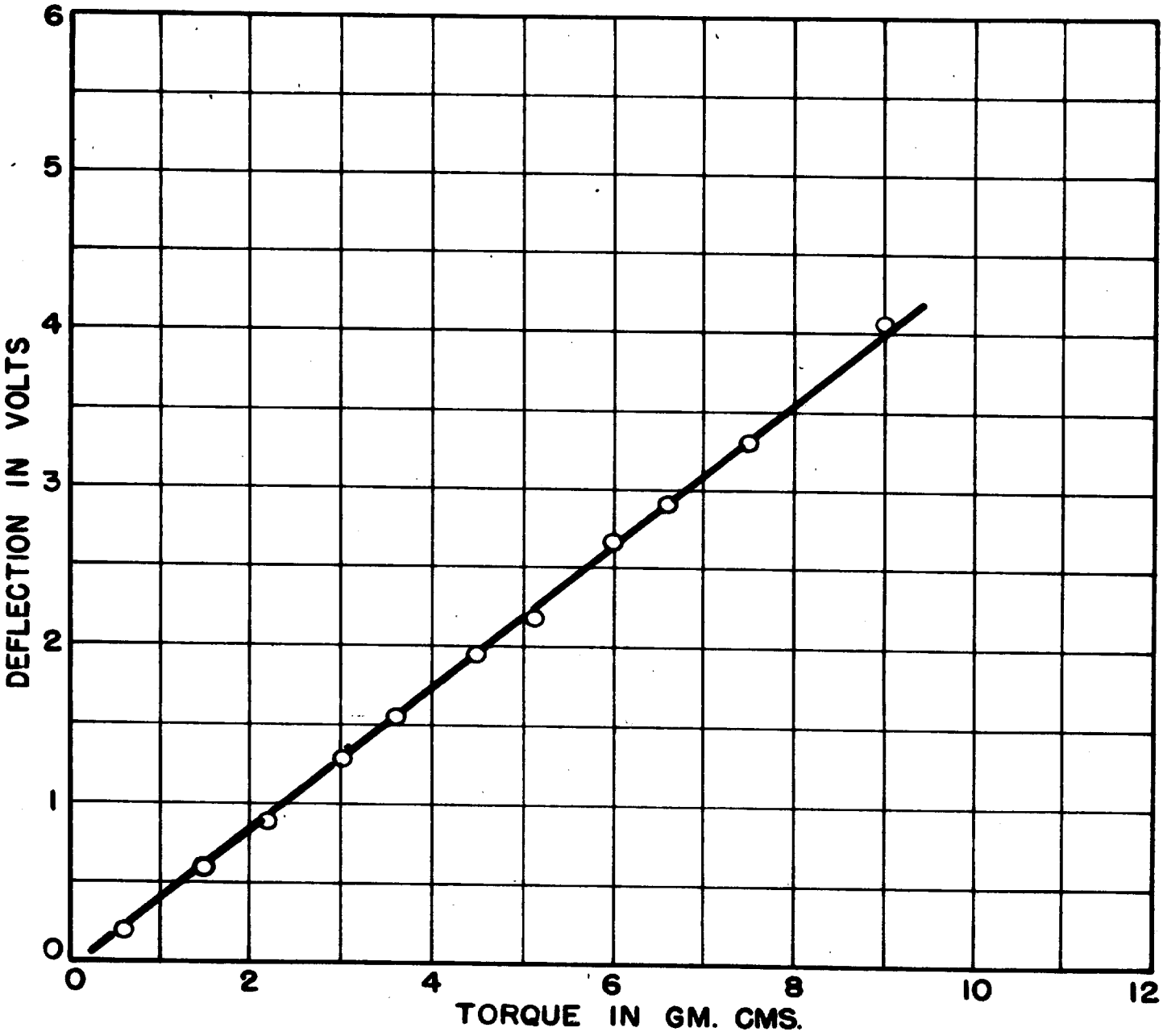

FIGURE 21

CALIBRATION CURVE OF ONE TUBE

TABLE 5

CALIBRATION OF TWO TUBES

Distance between springs and tube diaphragm = 1.5 cms

Force arm = 4 cms

Load gms.	Torque gm.cms.	Run 1 Voltage	Run 2 Voltage	Average Voltage
0.00	0.00	0.00	0.00	0.00
0.5144	2.05	0.9	1.15	1.025
0.7144	2.85	1.1	1.65	1.325
1.0144	4.05	2.05	2.1	2.075
1.2144	4.85	1.75	2.65	2.20
1.5144	6.05	3.2	3.35	3.275
1.7144	6.85	3.55	3.75	3.65
2.0144	8.05	4.00	4.3	4.15
2.2144	8.85	---	4.5	4.5

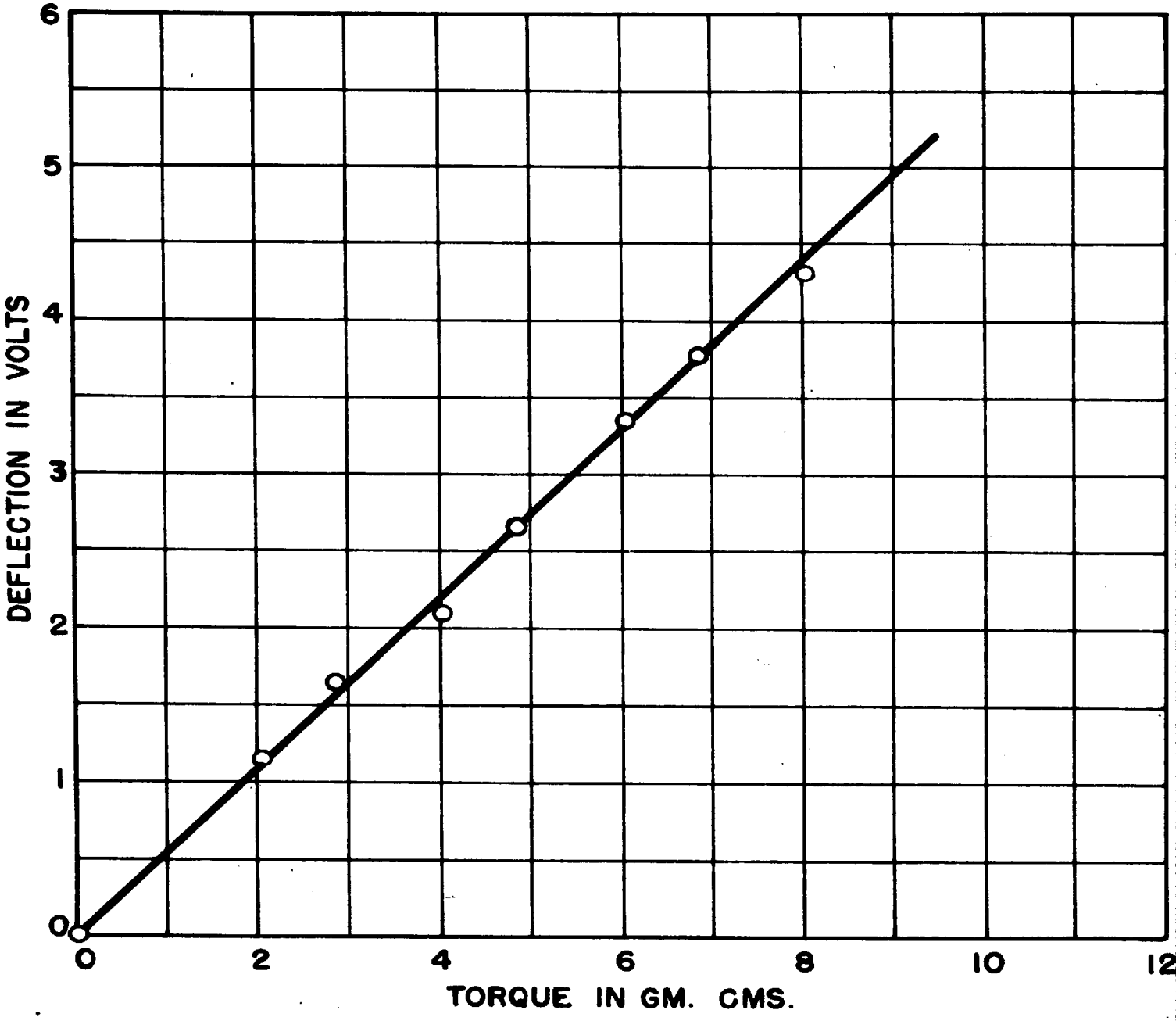

FIGURE 22

CALIBRATION CURVE OF TWO TUBES

Most of the tests carried out using this method were intended for comparison with the results obtained from the preceeding method. First, with the probe placed 0.55 inches under the nozzle and stationary at a particular point, the variations of the sheath thickness with variations of fuel pressure were recorded. This test was performed on nozzle Number 6702074 A 2/3 DED C52 four different times, and the results are included in Tables 6, 7, 8, and 9. In addition, the study of the variation of the thickness of the fuel sheath around its entire circumference was obtained by rotating the tube around in the spray at 1 r.p.m. Figures 23, 24, and 25 show the charts for the good nozzle, while Figure 26 shows the chart for the defaced nozzle. Figures 27 and 28 show the charts for nozzles that were in actual use on a jet engine. These last two charts were recorded using a 4 microfarad condenser across the input terminals of the d-c amplifier to by-pass the parasitic vibration currents.

Discussion of the Results:

The noise picked up by the oscillograph and shown in Figures 23, 24, 25, and 26 resulted from the vibrations of the mechanical system superimposed upon a 60 cycle pick up from the d-c amplifier. These charts, however, are clearer and more reproducible than those obtained by the strain gauge pick up.

The use of the condenser, however, cut out all these vibrations and the charts are clearer and can easily be examined,

as shown in Figure 27 and 28. This is at the expense of a small reduction in the sensitivity of the instrument which is compensated for by the use of a higher gain of the d-c amplifier.

Examining the charts for nozzle Number 6702074 A - 2/3 DED C52, shown in Figures 23, 24, and 25, it can be seen that they are uniform indicating that it is a good nozzle. In comparison, the chart for nozzle Number 6702074 A 3-29-48-5 DED C52 shown in Figure 26, shows that it is a damaged nozzle.

The charts in Figures 27 and 28 for nozzles Number 5230410 - 122A and 5230410 93A, respectively, represent typical examples of nozzles which have been in active use on an engine for fifty hours. The irregularities in these charts are believed to be caused by the carbon deposits on the tips of the nozzles resulting from constant use.

In reference to the results of the four tests on the nozzle Number 6702074 A - 2/3 DED C52, it is found that the sheath thickness of the spray varies with the pressure of the fuel. The sheath thickness decreases with pressure to a minimum at 250 psi and then rises again. The values, however, of the sheath thickness calculated at low pressures are not accurate. This results from the fluctuations in the flow rate meter readings caused by the instability of the high pressure pump at such low pressures.

TABLE 6

DATA ON SPRAY OF NOZZLE 6702074 A - 2/3 DED C 52

(R.C.A. TUBE)

a = 0.55 in.

No.	Press. in #/sq.in.	Discharge in #/hour	Voltage in Volts	Torque in gm.cms.	θ	Force arm in cms.	Force in Grams	Sheath Thick. b
1	50	78	0.225	0.65	36°-- '	2.30	---	---
2	100	154	0.450	1.10	36 --	2.30	0.477	0.0545
3	150	201	0.690	1.70	34 40	2.37	0.717	0.0650
4	200	240	1.000	2.40	32 40	2.51	0.957	0.0740
5	250	281	1.310	3.10	35 30	2.33	1.220	0.0660
6	300	318	1.650	3.80	36 15	2.32	1.630	0.0670
7	350	354	2.050	4.70	36 15	2.32	2.020	0.0820
8	400	385	2.500	5.70	32 30	2.39	2.380	0.0780
9	450	415	3.000	6.80	32 30	2.39	2.840	0.0760



TABLE 7

DATA ON SPRAY NOZZLE 6702074 A - 2/3 DED C52

(R.C.A. TUBE)

a = 0.55 in.

No.	Press. in #/sq.in.	Discharge in #/hour	Voltage in Volts	Torque in gm.cms.	θ	Force arm in cms.	Force in Grams	Sheath Thick. b
1	50	72	0.175	0.55	--°--'	---	---	---
2	100	148	0.400	1.00	36 --	2.30	0.435	0.0550
3	150	204	0.670	1.60	34 40	2.37	0.676	0.0705
4	200	240	0.970	2.30	32 40	2.51	0.920	0.0770
5	250	287	1.320	3.10	35 30	2.33	1.330	0.0685
6	300	322	1.650	3.80	36 15	2.32	1.645	0.0690
7	350	357	2.020	4.65	36 15	2.32	2.010	0.0680
8	400	387	2.450	5.60	32 30	2.39	2.350	0.0800
9	450	419	3.000	6.80	32 30	2.39	2.850	0.0765



TABLE 8

DATA ON SPRAY NOZZLE 6702074 A - 2/3 DED C52

(R.C.A. TUBE)

a = 0.55 in.

No.	Press. in #/sq.in.	Discharge in #/hour	Voltage in Volts	Torque in gm.cms.	θ	Force arm in cms.	Force in Grams	Sheath Thick. b
1	50	77	0.10	0.40	--°--'	---	---	---
2	100	151	0.35	0.90	36 --	2.30	0.392	0.0635
3	150	202	0.55	1.40	34 40	2.37	0.590	0.0790
4	200	237	0.85	2.05	32 40	2.51	0.820	0.0840
5	250	283	1.20	2.80	35 30	2.33	1.200	0.0715
6	300	319	1.52	3.55	36 15	2.32	1.530	0.0725
7	350	353	1.87	4.30	36 15	2.32	1.850	0.0730
8	400	388	2.37	5.40	32 30	2.39	2.260	0.0835
9	450	416	2.87	6.50	32 30	2.39	2.720	0.0800



TABLE 9

DATA ON SPRAY OF NOZZLE 6702074 A - 2/3 DED C52

(R.C.A. TUBE)

a = 0.55 in.

No.	Press. in #/sq.in.	Discharge in #/hour	Voltage in Volts	Torque in gm.cms.	θ	Force arm in cms.	Force in Grams	Sheath Thick. b
1	50	75	0.125	0.40	--°--'	---	---	---
2	100	154	0.420	1.10	36 --	2.30	0.477	0.0540
3	150	204	0.650	1.60	34 40	2.37	0.676	0.0710
4	200	238	0.920	2.25	32 40	2.51	0.900	0.0780
5	250	284	1.250	2.90	35 30	2.33	1.245	0.0700
6	300	322	1.570	3.65	36 15	2.32	1.575	0.0710
7	350	354	1.920	4.45	36 15	2.32	1.920	0.0705
8	400	389	2.400	5.45	32 30	2.39	2.280	0.0830
9	450	418	2.900	6.60	32 30	2.39	2.770	0.0790



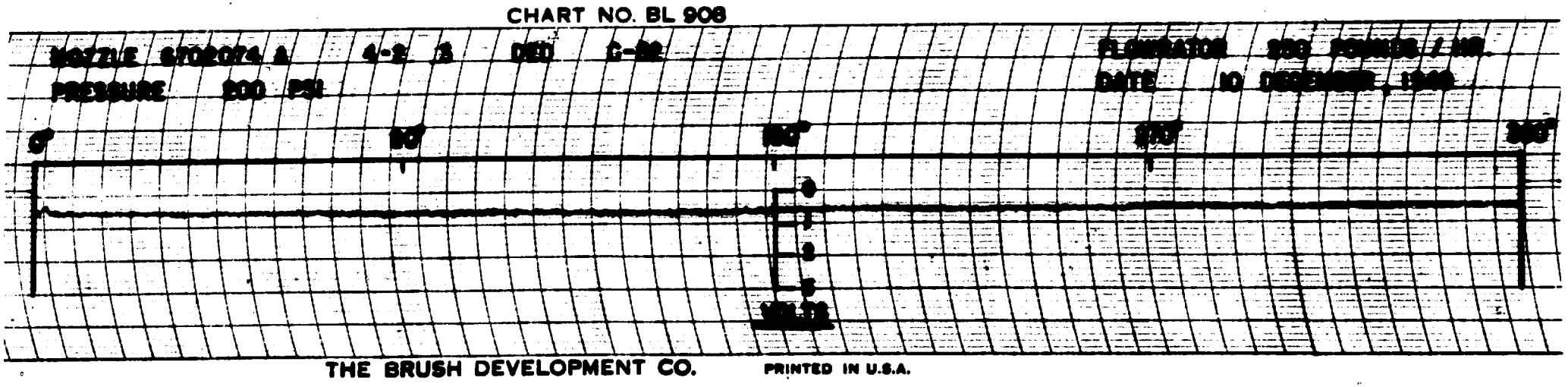

FIGURE 23

OSCILLOGRAPH CHART FOR SIMPLEX NOZZLE 6702074 A 4-2/3 DED C52

(TUBE)

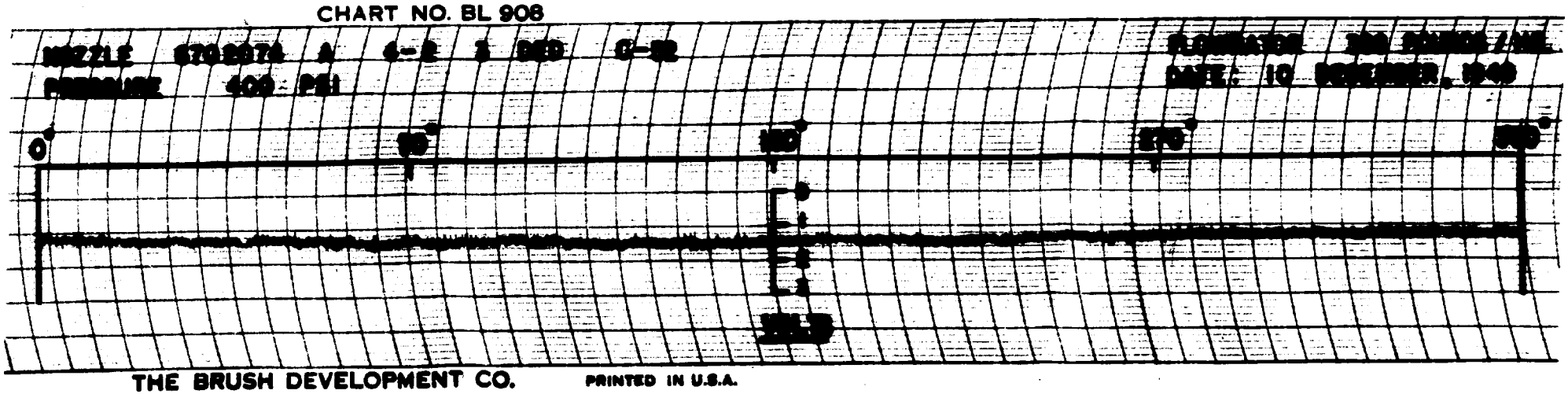

FIGURE 24

OSCILLOGRAPH CHART FOR SIMPLEX NOZZLE 6702074 A 4-2/3 DED C52

(TUBE)

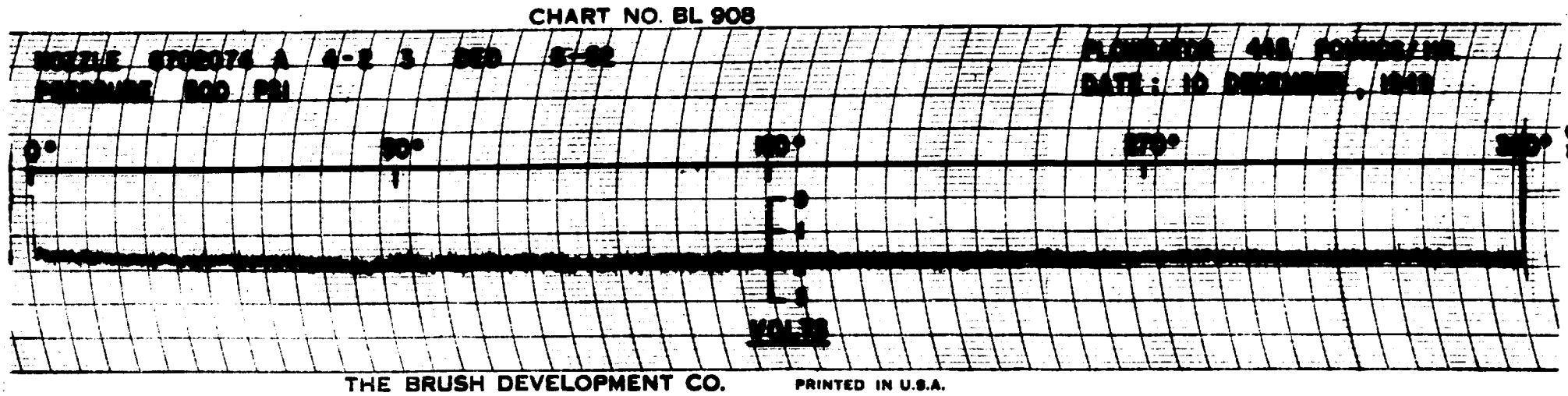

FIGURE 25

OSCILLOGRAPH CHART FOR SIMPLEX NOZZLE 6702074 A 4-2/3 DED C52

(TUBE)

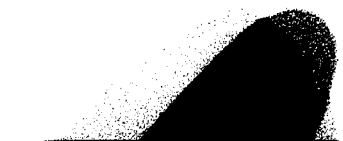

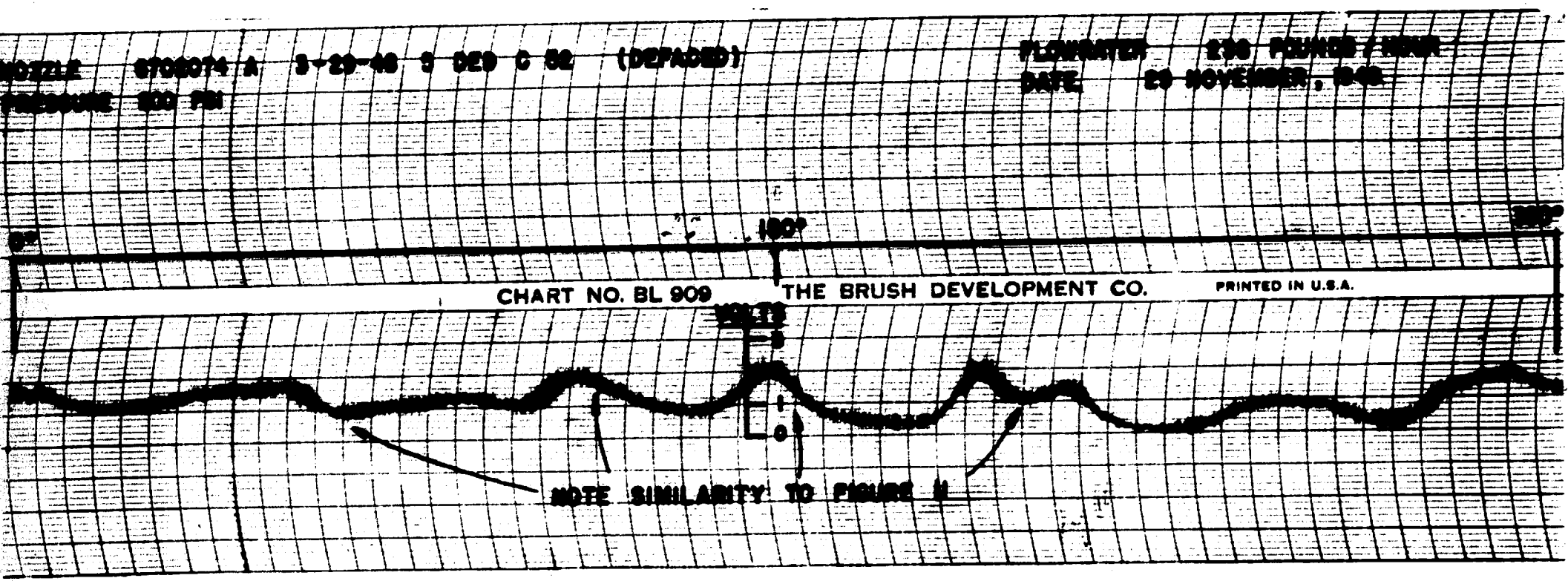

FIGURE 26

OSICLLOGRAPH CHART FOR DEFACED SIMPLEX NOZZLE 6702074 A 3-29-48 5 DED C52

(TUBE)



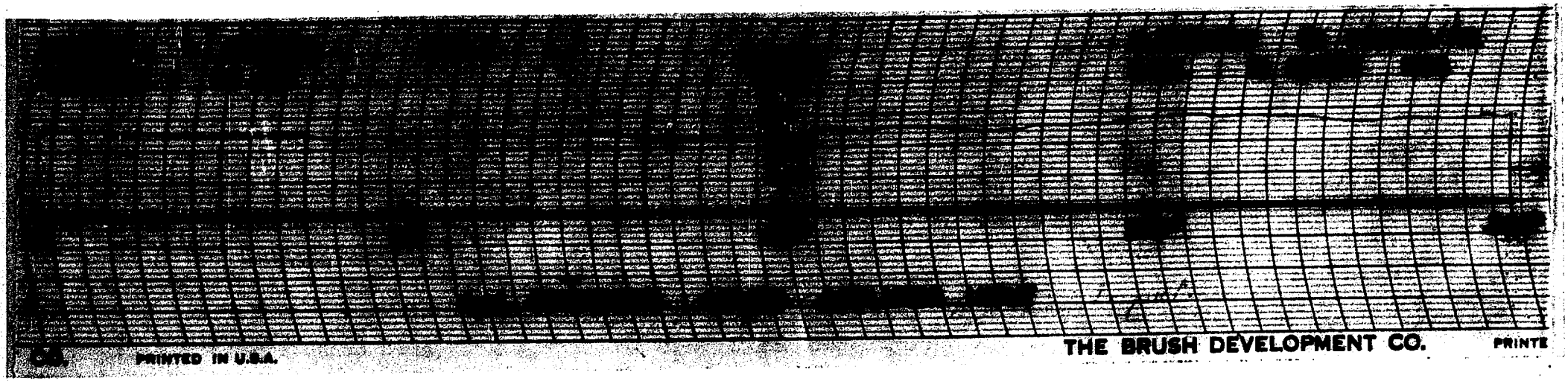

FIGURE 27

OSCILLOGRAPH CHART FOR SIMPLEX NOZZLE 5230410 122A
USING A 4 u.f. CONDENSER ACROSS AMPLIFIER INPUT

(TUBE)

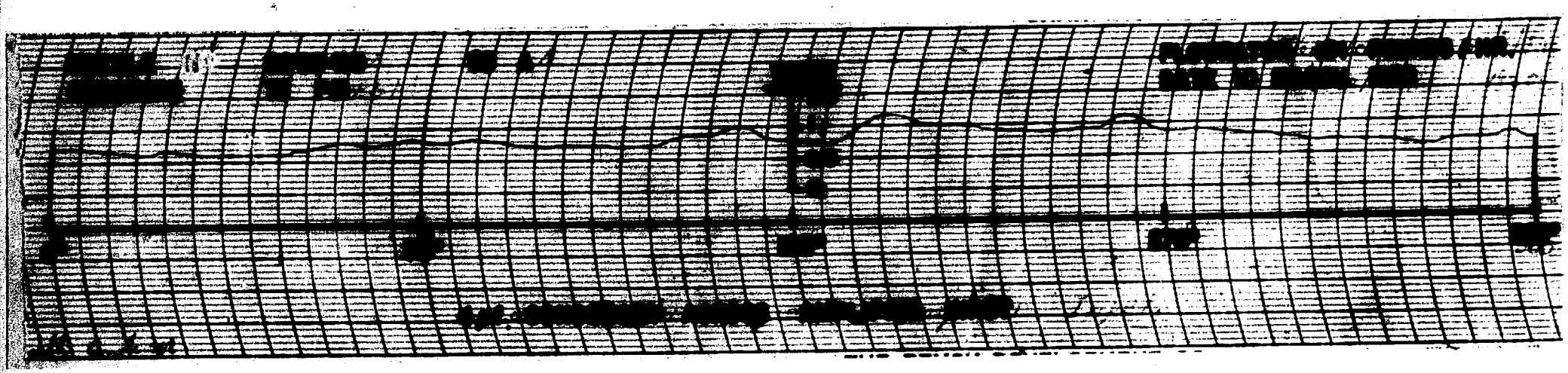

FIGURE 28

OSCILLOGRAPH CHART FOR SIMPLEX NOZZLE 5230410-93A
USING A 4 u.f. CONDENSER ACROSS AMPLIFIER INPUT

(TUBE)

CHAPTER III

OTHER METHODS

In the two experiments described above, the sheath thickness is determined by the measurement of the force in the spray. It is the purpose of further experimentation to devise a third means of measuring the sheath thickness by utilizing another physical property of the spray. This is felt to be desirable in order to compare with the results obtained by means of the first two methods.

Among the various methods considered are the following.

Absorption of Light

It is believed that by placing a point source of light on the axis of the conical sheath near the nozzle, the sheath thickness can be determined by the use of a photocell located outside the conical sheath as follows.

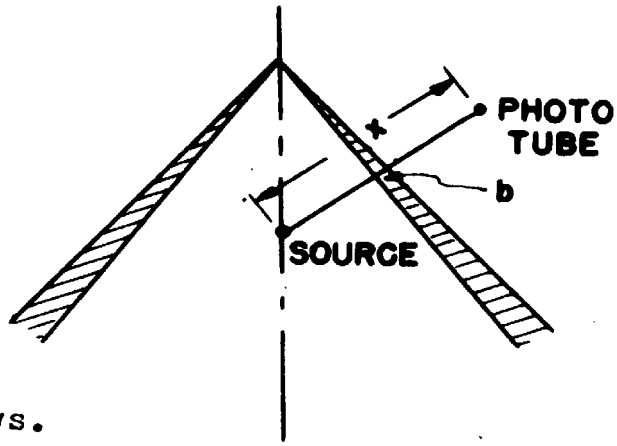

Let:

I_0 = Intensity of light at the source.

I_1 = Intensity of light at photo tube (no spray)

I_2 = Intensity of light at photo tube (with spray)

a_1 = Absorption factor of air

a_2 = Absorption factor of fuel

b = Sheath thickness

x = Distance between source and tube

Hence:

$$\frac{I_1}{I_0} = ke^{-a_1x}$$

$$\frac{I_2}{I_0} = ke^{-[a_1(x-b) + a_2b]}$$

$$= ke^{-[a_1x + b(a_2-a_1)]}$$

$$\therefore \frac{I_2}{I_1} = e^{-[a_1x + b(a_2-a_1) - a_1x]}$$

$$= e^{-b(a_2-a_1)}$$

By introducing sheaths of fuel of known thicknesses between the point source and the photo tube, calibration curves can be obtained for b versus I_1/I_2 from which b can easily be found.

This method may seem practical but its application to this problem is difficult and inaccurate because of the following reasons:

1. Since the oil picks up dirt from the oil tank, the pumps, and the pipe lines, its absorption factor changes considerably.
2. There are many loose drops in the spray chamber moving in every direction between the source and the photo tube while the nozzle is in operation. The accumulation of these drops is dependent upon the oil pressure. This so-called fog is an important source of error in the estimation of the thickness of the sheath between the source and the tube.

The combination of these factors made further experimentation along this line impractical.

Radioactivity

Since radioactivity has been successfully used for measuring the thickness of thin metallic sheets, its applicability to this case is considered. It is thought that by introducing some phosphorus compound into the fuel in order to make it radioactive, sheath thickness can then be determined by placing a Geiger counter outside the conical sheath to measure the radioactivity. This was found inadequate and would yield inaccurate results because of the following considerations:

1. The counter indicates the radioactivity within that portion of the sheath falling within a solid angle with the counter as the apex. Therefore the readings of the counter are not directly proportional to the sheath thickness.

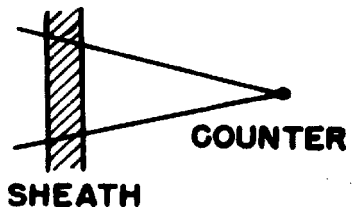

2. Since the counter readings are proportional to the amount of radioactivity of the fuel passing the counter, a thick sheath moving at a low velocity v_1 would give the same number of counts as a thinner sheath moving at a higher velocity v_2 providing that $\frac{b_1}{b_2} = \frac{v_2}{v_1}$
3. The effect of the loose drops in the spray chamber is an additional source of error as in the absorption of light case.
4. Finally, aside from all the above considerations,

there is grave danger to personnel since any leakage of the radioactive drops outside the spray chamber might be fatal.

The points mentioned above discouraged any further consideration of the use of radioactivity in connection with this problem. Only if some means is devised whereby a single drop of radioactive fuel can be sampled from the spray chamber, will the application of radioactivity to fuel spray study be possible. If this is done, the drop size can be obtained as follows:

$$\frac{\text{Volume of drop}}{\text{Volume of the fuel}} = \frac{\text{Radioactivity in the drop}}{\text{Radioactivity of whole fuel}}$$

Capacitance:

Another method considered by which the sheath thickness could be determined was the use of a narrow parallel plate capacitor mounted as shown in the accompanying figure. The thickness of the sheath can be calculated by the change in capacitance as follows:

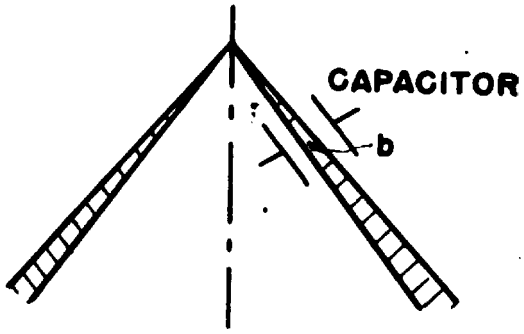

The differential equation for the voltage V at any point x of the parallel plate capacitor shown in the opposite figure is

$$\nabla^2 V = 0$$

$$\frac{\partial^2 V}{\partial x^2} = 0$$

$$V = Ax + B$$

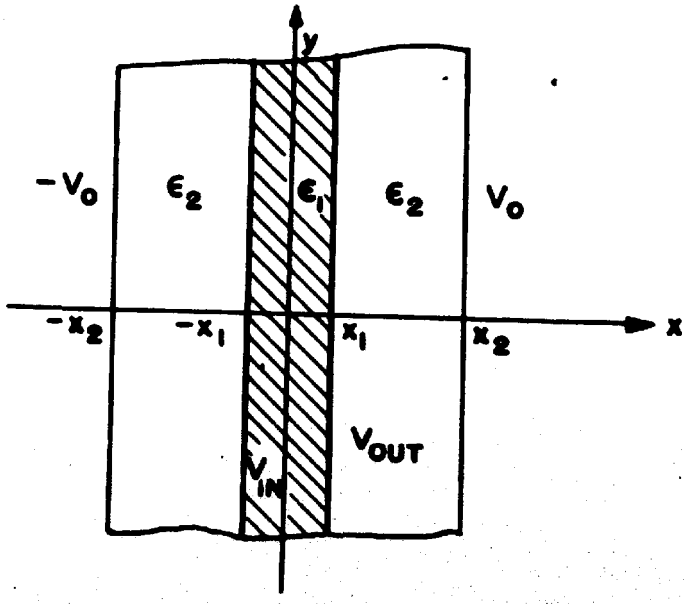

Inside:

$$V = 0 \text{ at } x = 0$$

$$V_{in} = Ax$$

Outside:

$$V = V_0 \quad \text{at} \quad x = x_2$$

$$\therefore V_0 = Bx_2 + M$$

$$\therefore M = V_0 - Bx_2$$

$$\therefore V = Bx + V_0 - Bx_2$$

$$\therefore V_{out} = V_0 + B(x-x_2)$$

$$V_{out} = V_0 - B(x_2-x)$$

Boundary Conditions;

$$\text{at } x = x_1 \qquad V_{out} = V_{in}$$

$$\text{at } x = x_1 \qquad D_N(out) = D_N(in)$$

$$\therefore Ax_1 = V_0 - B(x_2-x_1)$$

$$D_N(in) = -\epsilon_1 A$$

$$D_N(out) = -\epsilon_2 B$$

$$\therefore A = \frac{\epsilon_2 B}{\epsilon_1}$$

$$\therefore \frac{\epsilon_2 B}{\epsilon_1} x_1 = V_0 - B(x_2-x_1)$$

$$\therefore \epsilon_2 B x_1 = V_0 \epsilon_1 - \epsilon_1 B x_2 + \epsilon_1 B x_1$$

$$\therefore B(\epsilon_2 x_1 + \epsilon_1 x_2 - \epsilon_1 x_1) = V_0 \epsilon_1$$

$$B = \frac{V_0 \epsilon_1}{\epsilon_2 x_1 + \epsilon_1 x_2 - \epsilon_1 x_1}$$

$$\therefore A = \frac{V_0 \epsilon_2}{\epsilon_2 x_1 + \epsilon_1 x_2 - \epsilon_1 x_1}$$

$$\therefore V_{in} = \frac{V_0 \epsilon_2}{\epsilon_2 x_1 + \epsilon_1 x_2 - \epsilon_1 x_1} x$$

$$V_{out} = V_0 - \frac{V_0 \epsilon_1}{\epsilon_2 x_1 + \epsilon_1 x_2 - \epsilon_1 x_1} (x_2 - x)$$

$$D_N = -\epsilon_1 A$$

$$= - \frac{\epsilon_2 \epsilon_1 V_0}{\epsilon_2 x_1 + \epsilon_1 x_2 - \epsilon_1 x_1}$$

$$Q = - \frac{A \epsilon_2 \epsilon_1 V_0}{\epsilon_2 x_1 + \epsilon_1 x_2 - \epsilon_1 x_1}$$

Capacity $C_d = \frac{Q}{2V_0}$

$$C_d = \frac{A \epsilon_2 \epsilon_1}{2(\epsilon_2 x_1 + \epsilon_1 x_2 - \epsilon_1 x_1)}$$

$$C_p = \frac{\epsilon_2 A}{2x_2}$$ (Parallel plate only)

$$\frac{C_p}{C_d} = \frac{\epsilon_2 A(\epsilon_2 x_1 + \epsilon_1 x_2 - \epsilon_1 x_1)}{2x_2 \epsilon_2 \epsilon_1 A}$$

$$\frac{C_p}{C_d} = \frac{1}{\epsilon_1 x_2} (\epsilon_2 x_1 + \epsilon_1 x_2 - \epsilon_1 x_1)$$

$$\frac{C_p}{C_d} = 1 - \frac{x_1}{x_2}(1 - \frac{\epsilon_2}{\epsilon_1})$$

Thus by measuring C_p and C_d and substituting for ϵ_1, ϵ_2, and x_2 in the above equation, the value of x_1 can be calculated. The average sheath thickness between the plates of the capacitor is $b = 2x_2$

The following numerical example shows the dimensions and capacitance of a typical parallel plate capacitor suitable for the measurement of spray sheath thickness.

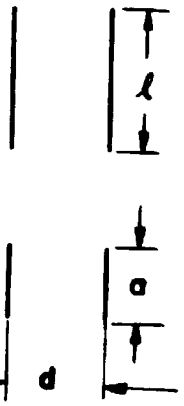

$b = 0.075$ inches (typical value taken from results of previous tests)

$x_1 = 0.0375$ inches

$d = 0.2$ inches

$x_2 = 0.1$ inches

$\ell = 0.3$ inches

$f = 0.2$ inches

$$\epsilon_2 = \epsilon_0 = \frac{10^{-9}}{36\pi}$$

$$\epsilon_1 = \epsilon_r \epsilon_0 = 4\epsilon_0 \text{ (for kerosene)}$$

$$C_p = \frac{\epsilon_2 \ell f}{d}$$

$$= \frac{0.2 \times 0.3 \times (2.54)^2 \times 10^{-11}}{36 \times \pi \times 0.2 \times 2.54}$$

$$= 0.0672 \quad \mu\mu f.$$

$$\frac{C_p}{C_d} = 1 - \frac{x_1}{x_2}\left(1 - \frac{\epsilon_2}{\epsilon_1}\right)$$

$$\frac{C_p}{C_d} = 1 - \frac{0.0375}{0.1}\left(1 - \frac{1}{4}\right)$$

$$= 0.719$$

$$C_d = \frac{0.0672}{0.719} = 0.094 \quad \mu\mu f.$$

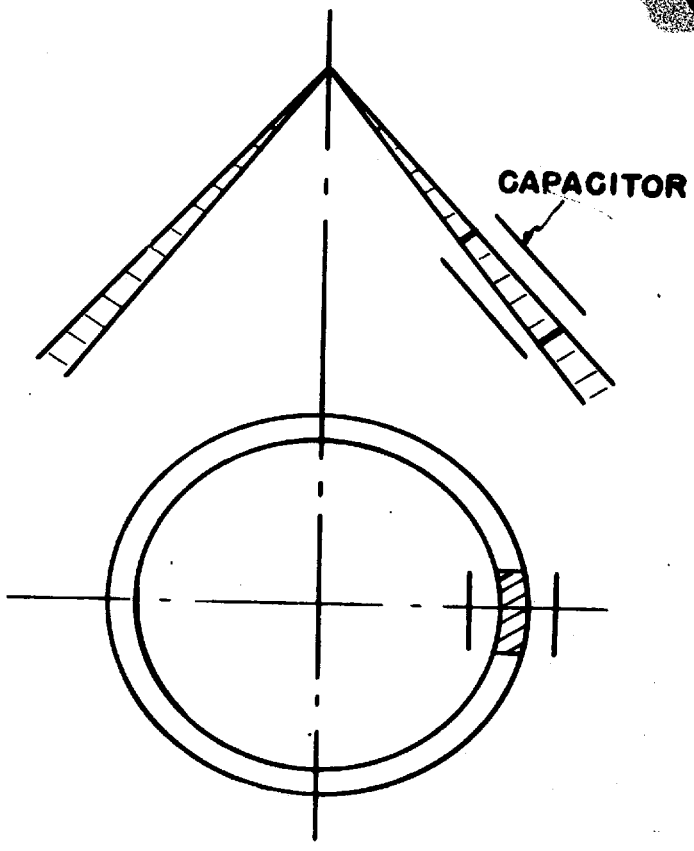

However, this method is impractical in this case for the following reasons:

1. The initial capacitance of the parallel plate capacitator is very small; therefore a very sensitive bridge is required to measure the change in capacitance caused by the passage of the sheath between the plates. Such a bridge is difficult, if not impossible, to construct.
2. In addition, the leads between the capacitor and the bridge circuit will have a capacitance of the same or even greater magnitude than that of the capacitor itself. This will make the measurements highly inaccurate and impose a further problem of devising more suitable means of connecting the capacitor to the bridge.
3. Finally, the capacitor must be rotated in order to study the circumferential characteristics of the sheath. This process would require elaborate mechanical mountings since the most minute change in the spacing between the plates would have a large effect upon the capacitance. Such a mounting is difficult to construct.

Hence, this method is also discarded for use at the present time.

CONCLUSIONS

From study of the previous experiments, several conclusions may be drawn. First, the most successful method of measuring the sheath thickness of the spray appears to be that which utilizes the measurement of the force of the spray. As can be seen from an examination of the other methods considered, the other physical properties of the spray do not lend themselves so readily to an accurate and practical method of spray analysis. In these cases, either the analysis would not be reliable and reproducible, or elaborate, expensive or unavailable equipment would be needed.

Comparing the results obtained by the use of the strain gauge with those obtained by the use of the tube, it can be seen that each is better suited for a particular range of pressures. Since the strain gauge set up is more durable, it can be more easily accommodated to measurements at high fuel pressures. However, at low pressures it tends to be less accurate. Another advantage of the strain gauge set up is its compactness, which allows it to be easily installed in experimental combustion chambers.

On the other hand, the tube arrangement is more sensitive in the low and medium pressure ranges. However, at high pressures the deflection of the plate shaft of the tube caused by the force of the spray is too great, forcing the tube out of range and destroying it. This can be avoided by the use of heavier springs, but only at the sacrifice of some of the sensitivity of the instrument. Advantages of the tube device may

be seen in the reproducibility of the charts obtained, and its comparative immunity to fatigue. Thus, there are advantages and disadvantages in the use of both methods described herein. However, since in actual jet engine construction the tendency at present is toward the application of high pressures to the fuel, the strain gauge method, which is durable at these high pressures, would be recommended for the testing of currently designed nozzles.

There are six qualities mentioned in the introduction which should be present in an ideal fuel spray analyzer. These are: rapidity, ability to give quantitative information regarding the mass distribution of the spray cone and mean drop size, compactness, non-interference with the air-fuel flow, ability to determine to what extent a set of nozzles is matched at all fuel pressures, and finally, the ability to yield permanent graphical records.

It can be seen that the two methods herein described correspond in all important respects with the above characteristics. The slight interference with the normal air-fuel flow is reduced to a minimum by the use of only a thin wire as a probe to be inserted into the spray sheath. These methods do not provide a means for determining the drop sizes in the spray. However, the instrument approaches the ideal analyzer more closely than has hitherto been reported.

The U. S. Army Air Materiel Command has sent many simplex and duplex nozzles previously tested by the patternator to be tested by these methods. Some nozzles were new, others had

been in actual use in aircraft engines. Some had been causing hot spots in the combustion chamber of the engines. These imperfect nozzles were easily distinguished from the others. The results of the tests on these nozzles by either of the two methods were found to correlate exactly with the results obtained by the use of the patternator or other more complicated tests. It is felt that the rapidity and accuracy of these testing methods can be of great service to jet engine development and research. Already, plans are under way to make these the standard industrial methods for testing fuel spray nozzles.

APPENDIX I

Sample of Calculations

Sample of Calculations

Pressure = 250 lbs./sq.in.

Discharge = 290 lbs./hour

$c = 0.15"$

$\text{Tan}\theta = \frac{0.5}{0.7} = 0.715$

$\text{Cos}\theta = 0.815$

$\text{Sin}\theta = 0.582$

$\Delta = 0.5"$

$E = 16 \times 10^6$ lbs./sq.in.

$f = 0.25"$

$h = 0.01"$

$\text{Strain} = \frac{Bh}{2EI}$

$= \frac{12Bh}{2Efh^3}$

$= \frac{6B}{Efh^2}$

If B is in lbs. inches

S in inches/inch

$S = \frac{6B}{Efh^2}$ inches/inch

$= \frac{6B}{16 \times 10^6 \times 0.25 \times (0.01)^2}$ inches/inch

$= \frac{6B \times 10^6}{16 \times 10^6 \times 0.25 \times 10^{-4}}$ μ inches/inch

$B = \frac{4 \times 10^{-4}}{6} S$

$B = 66.6 \times 10^{-6} S$ lbs.inches

S in this case = 108 μ inches/inch

$B = 66.6 \times 10^{-6} \times 108 = 7.2 \times 10^{-3}$ lbs. inches

but $B = F \times \ell \times \cos\theta + F \times c \times \sin\theta$

$\ell = L - \Delta = 3.105 - 0.5 = 2.605$ inches

$\therefore 7.2 \times 10^{-3} = F \times 0.815 \times 2.605 + F \times 0.582 \times 0.15$

$7.2 \times 10^{-3} = F(2.12 + 0.0874)$

$$F = \frac{7.2 \times 10^{-3}}{2.2074} = 3.265 \times 10^{-3} \text{ lbs.}$$

$= 3.265 \times 453.6 \times 10^{-3}$

$= 1.48$ grams

From Equation (5) we get

$$b = \frac{Q^2 w}{2\pi a g F \tan\theta}$$

$$Q = \frac{290}{50} = 5.8 \text{ cu.ft./hr.}$$

$$= \frac{5.8}{60 \times 60} \text{ cu.ft./sec.}$$

$w = 50$ lbs./cu.ft. for kerosene at room temperature 70° F.

$g = 32$ ft./sec./sec.

$a = 0.55"$

$$\therefore b = \frac{(5.8)^2 \times 50 \times 12 \times 12}{(60 \times 60)^2 \times 2\pi \times 0.55 \times 3.265 \times 10^{-3} \times 0.715 \times 32 \times 12}$$

$= 0.072"$

APPENDIX II

Exact Calculation of Force in Spray

Exact Calculation of Force in Spray

In this procedure the force in the spray is calculated without the assumption of a continuous sheath leaving the nozzle.

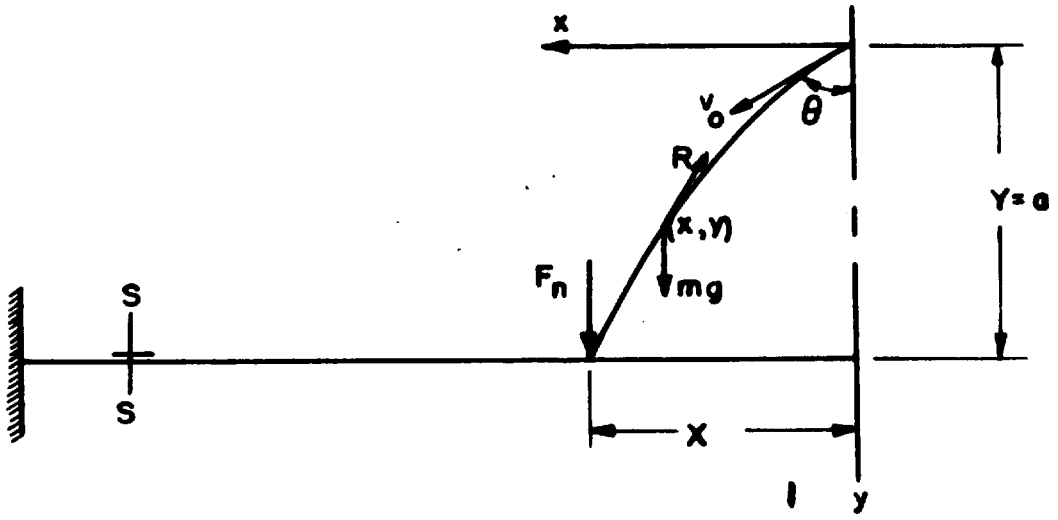

Let

m = mass of mean drop size

v_o = mean drop discharge velocity

θ = 1/2 spray angle

Assume the force of resistance to the motion of the drop is proportional to the square of the drop velocity, i.e.

$$R = k_1 v^2$$

$$R_x = k_1 v_x^2 = k_1 \left(\frac{dx}{dt}\right)^2$$

$$R_y = k_1 v_y^2 = k_1 \left(\frac{dy}{dt}\right)^2$$

The differential equation of motion in the x direction is

$$m \frac{d^2x}{dt^2} = -R_x = -k_1 \left(\frac{dx}{dt}\right)^2$$

$$\therefore \frac{dx^2}{dt^2} + \frac{k_1}{m} \left(\frac{dx}{dt}\right)^2 = 0$$

or $\frac{dx^2}{dt^2} + k\left(\frac{dx}{dt}\right)^2 = 0$ $\qquad \left(k = \frac{k_1}{m}\right)$

this can be written as

$$\frac{dv_x}{dt} = -kv_x^2$$

$$\therefore \frac{dv_x}{v_x^2} = -k\,dt$$

$$\therefore \int_{v_{ox}}^{v_x} \frac{dv_x}{v_x^2} = -k\int_o^t dt$$

$$\therefore \left[-\frac{1}{v_x}\right]_{v_{ox}}^{v_x} = -kt$$

$$\therefore \frac{1}{v_{ox}} - \frac{1}{v_x} = -kt$$

$$\therefore v_x = \frac{dx}{dt} = \frac{v_{ox}}{kv_{ox}t + 1} \qquad (v_{ox} = v_o\sin\theta)$$

Separating variables, we get

$$dx = \frac{v_{ox}dt}{kv_{ox}t + 1}$$

$$\therefore \int_o^x dx = v_{ox}\int_o^t \frac{dt}{1 + kv_{ox}t}$$

$$\therefore x = \frac{1}{k}\log(1 + kv_{ox}t)$$

or

$$x = \frac{m}{k_1}\log\left(1 + \frac{k_1 v_o\sin\theta}{m}\,t\right)$$

The differential equation of motion in the y direction is

$$m \frac{d^2y}{dt^2} = mg - R_y = mg - k_1 \left(\frac{dy}{dt}\right)^2$$

$$\therefore \frac{d^2y}{dt^2} = g - k \left(\frac{dy}{dt}\right)^2$$

This can be written as

$$\frac{dv_y}{dt} = g - kv_y^2$$

Separating variables we get

$$\frac{dv_y}{g - kv_y^2} = dt$$

$$\therefore \frac{g\, dv_y}{g^2 - kgv_y^2} = dt$$

Integrating, we get

$$\frac{1}{k} \frac{1}{2\sqrt{\frac{g}{k}}} \log \frac{\sqrt{\frac{g}{k}} + v_y}{\sqrt{\frac{g}{k}} - v_y} = t + C$$

$$\therefore \frac{1}{2\sqrt{gk}} \log \frac{g + \sqrt{kg}\, v_y}{g - \sqrt{kg}\, v_y} = t + C$$

$$\frac{g + \sqrt{kg}\, v_y}{g - \sqrt{kg}\, v_y} = C_1 e^{2\sqrt{kg}\, t}$$

When $t = 0$, $v_y = v_{oy}$ $\qquad (v_{oy} = v_o \cos\theta)$

$$\therefore C_1 = \frac{g + \sqrt{kg}\, v_{oy}}{g - \sqrt{kg}\, v_{oy}}$$

$$\therefore \frac{g + \sqrt{kg}\, v_y}{g - \sqrt{kg}\, v_y} = \frac{g + \sqrt{kg}\, v_{oy}}{g - \sqrt{kg}\, v_{oy}} e^{2\sqrt{kg}\, t}$$

Solving for v_y, we get

$$v_y = \frac{dy}{dt} = \sqrt{\frac{g}{k}} \frac{C_1 e^{2\sqrt{kg}\, t} - 1}{C_1 e^{2\sqrt{kg}\, t} + 1}$$

Integrating we get

$$y = \frac{1}{k} \log(C_1 e^{\sqrt{kg}\, t} + e^{\sqrt{kg}\, t}) + C_2$$

To determine C_2 we use the fact that at $t = 0$, $y = 0$

$$\therefore 0 = \frac{1}{k} \log(C_1 + 1) + C_2$$

$$\therefore C_2 = -\frac{1}{k} \log (C_1 + 1)$$

$$\therefore y = \frac{1}{k} \left[\log \left\{ C_1 e^{\sqrt{kg}\, t} + e^{-\sqrt{kg}\, t} \right\} - \log(C_1 + 1) \right]$$

$$= \frac{1}{k} \log \frac{C_1 e^{\sqrt{kg}\, t} + e^{-\sqrt{kg}\, t}}{C_1 + 1}$$

$$y = \frac{m}{k_1} \log \frac{C_1 e^{\sqrt{\frac{k_1 g}{m}}\, t} + e^{-\sqrt{\frac{k_1 g}{m}}\, t}}{C_1 + 1}$$

Let m = mean drop size (mass) grams

n = no. of drops/cu.cm.

ρ = density of spray

ρ = nm gm./cm.^{3}

v_y = velocity of drops perpendicular to wire

We assume that there is no friction between the wire and the spray and that there is no change in momentum along the wire.

Change in momentum of a drop = $m v_y$

Total change in momentum/cm.^{3} of liquid hitting the wire = $nm v_y$.

Quantity of liquid hitting wire/sec.

= $Av = bdv$ cm.^{3}

$\therefore$ Total change in momentum/sec. of liquid striking the wire = $nmbdv v_y$

$\therefore F_n = nmbdv v_y$

$= \rho bdv v_y$

$= \rho bd v_y \sqrt{(v_y)^2 + (v_x)^2}$

$= \rho bd\sqrt{\frac{g}{k}} \frac{C_1 e^{2\sqrt{kg}\, t} - 1}{C_1 e^{2\sqrt{kg}\, t} + 1}$

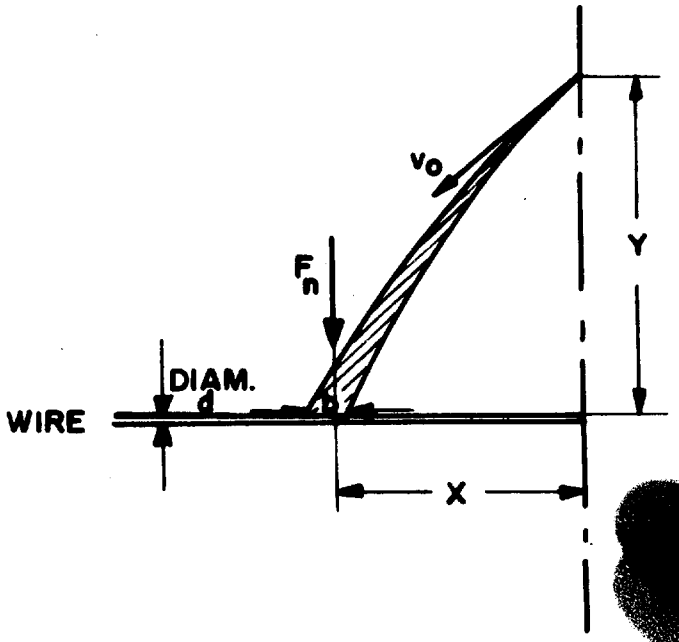

$$\sqrt{\left\{\sqrt{\frac{g}{k}}\left[\frac{C_1 e^{2\sqrt{kg}\, t} - 1}{C_1 e^{2\sqrt{kg}\, t} + 1}\right]\right\}^2 + \left\{\frac{v_o \sin\theta}{\frac{k_1}{m} t\, v_o \sin\theta + 1}\right\}^2}$$

Substituting for k by $\frac{k_1}{m}$ we get

$$F_n = \rho bd\sqrt{\frac{mg}{k_1}} \left\{\frac{C_1 e^{2\sqrt{\frac{k_1 g}{m}}\, t} - 1}{C_1 e^{2\sqrt{\frac{k_1 g}{m}}\, t} + 1}\right\}$$

$$\sqrt{\left\{\sqrt{\frac{mg}{k_1}}\left[\frac{C_1 e^{2\sqrt{\frac{k_1 g}{m}}\, t} - 1}{C_1 e^{2\sqrt{\frac{k_1 g}{m}}\, t} + 1}\right]\right\}^2 + \left\{\frac{v_o \sin\theta}{\frac{k_1}{m} t\, v_o \sin\theta + 1}\right\}^2}$$

We have

$$F_n = nmbdv\ v_y$$
$$= M\ v_y$$

M = mass of liquid striking the wire/sec.

$$M = F_n / v_y$$

Angle subtended by wire at the center of circle with axis of nozzle as center (tip of wire under axis of nozzle)

$$\beta = \frac{d}{2\pi x} 360^o$$

Mass of liquid going through a circumferential arc subtending one degree at center

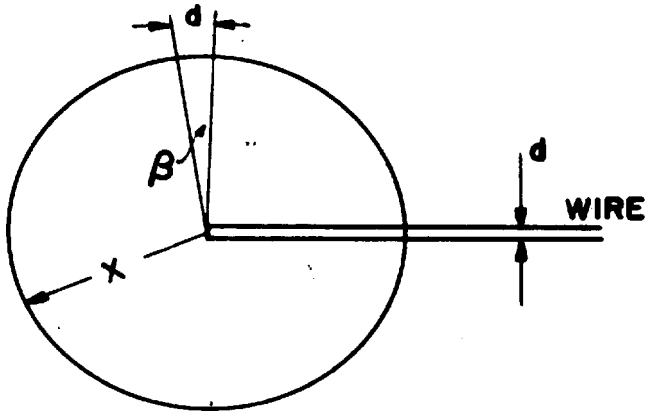

$$M_1 = \frac{M}{\beta} = \frac{F_n\ 2\pi x}{v_y\ 360\ d}$$

$$M_1 = \frac{2\pi F_n}{360 d} \sqrt{\frac{m}{k_1 g}} \left[\frac{C_1\ e^{2\sqrt{\frac{k_1 g}{m}}\ t} + 1}{C_1\ e^{2\sqrt{\frac{k_1 g}{m}}\ t} - 1} \right] \log \left[\frac{k_1}{m} v_o \sin\theta + 1 \right]$$

Q = amount of fuel coming out of nozzle/sec.

$$= \int_0^{360} M_1\, d\beta = \text{Area under the } M_1 - \beta \text{ curve}$$

$$F_n = \rho\, bd \sqrt{\frac{mg}{k_1}} \left\{ \frac{C_1 e^{2\sqrt{\frac{k_1 g}{m}}\, t} - 1}{C_1 e^{2\sqrt{\frac{k_1 g}{m}}\, t} + 1} \right\}$$

$$\sqrt{\left\{ \sqrt{\frac{mg}{k_1}} \frac{C_1 e^{2\sqrt{\frac{k_1 g}{m}}\, t} - 1}{C_1 e^{2\sqrt{\frac{k_1 g}{m}}\, t} + 1} \right\}^2 + \left\{ \frac{v_o \sin\theta}{\frac{k_1}{m} t\, v_o \sin\theta + 1} \right\}^2}$$

F_n can be found from the readings of the strain as recorded by the strain gauge.

Since

$$y = \frac{m}{k_1} \log \frac{C_1 e^{\sqrt{\frac{k_1 g}{m}}\, t} + e^{-\sqrt{\frac{k_1 g}{m}}\, t}}{C_1 + 1}$$

$$C_1 = \frac{g + \sqrt{kg}\, v_{oy}}{g - \sqrt{kg}\, v_{oy}}$$

Assuming a value for m and k_1 and the velocity v_o and measuring β we can get C_1 and knowing the distance $(y = a)$ between the nozzle and the wire we can find $t = t_1$.

Knowing F_n at a certain pressure then we can find b.

For a certain time $t = t_1$

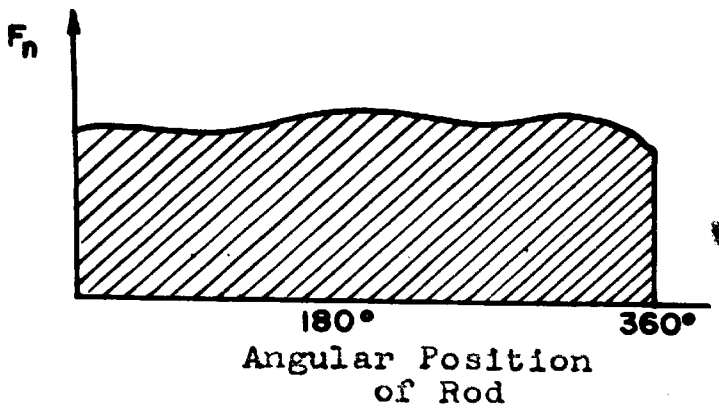

$M_1 = C\ F_n$

$$\therefore\ Q = \int_o^{360} C\ F_n\ d\beta$$

$$= C \int_o^{360} F_n\ d\beta$$

= C times area under F_n curve.

But the bending moment at s - s caused by F_n

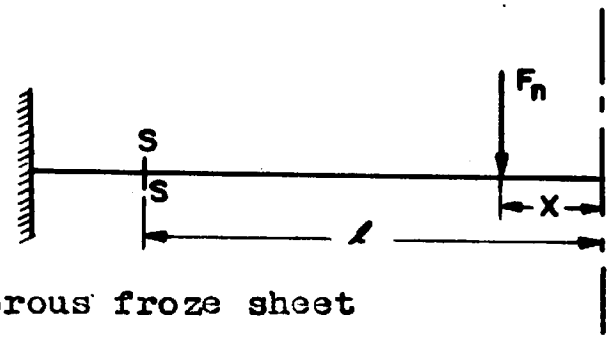

$$= F_n\ (\ell - x)$$

Strain in the upper fibre of the phosphorous froze sheet recorded by the strain gauge

$$S = \frac{F_n\ (\ell - x)}{EI}\ \frac{h}{2}$$

$\therefore$ For a certain fixed pressure and discharge through the nozzle, x is fixed. $\therefore$ S is proportional to F_n.

$$\therefore\ Q = k\int_o^{2\pi} S\ d\beta$$

= k times area under strain curve.

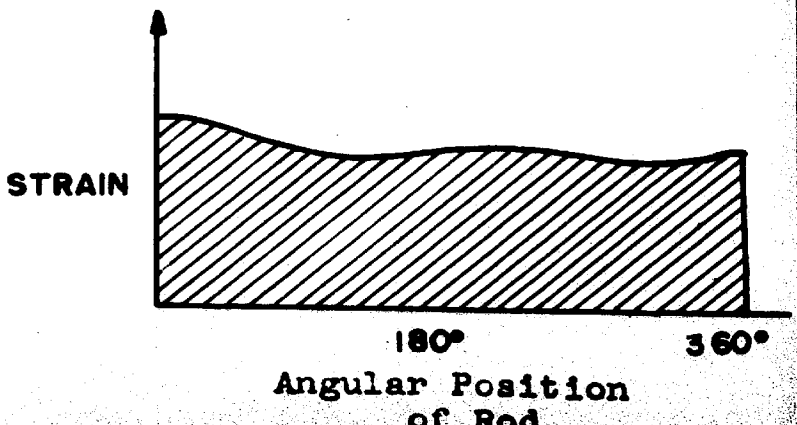

APPENDIX III

Sensitivity of Two Tubes in Comparison to One Tube

Sensitivity of Two Tubes in Comparison to One Tube

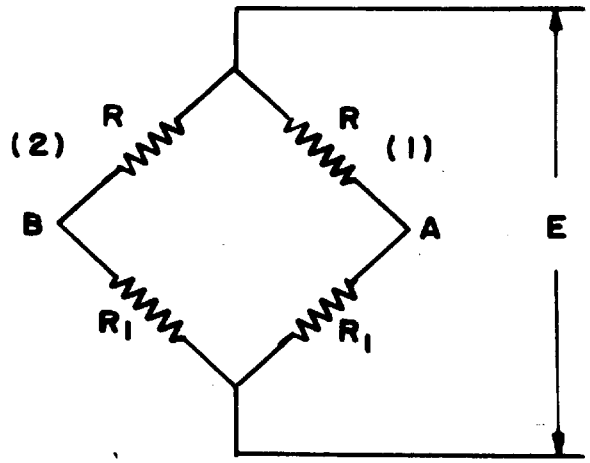

With the bridge balanced

$$E_{AB} = 0$$

Let R_{1A} change to $(R_1 + \Delta R)$

$$\therefore I_1 = \frac{E}{R + R_1 + \Delta R}$$

$$I_2 = \frac{E}{R + R_1}$$

$$E_A = \frac{ER}{R + R_1 + \Delta R} = \frac{E}{1 + \frac{R_1 + \Delta R}{R}}$$

$$E_B = \frac{E}{1 + \frac{R_1}{R}}$$

$$E_{AB} = E \frac{1 + \frac{R_1}{R} + \frac{\Delta R}{R} - 1 - \frac{R_1}{R}}{(1 + \frac{R_1}{R})(1 + \frac{R_1}{R} + \frac{\Delta R}{R})}$$

$$= \frac{E\,\Delta R}{(1 + \frac{R_1}{R})(R + R_1 + \Delta R)}$$

But ΔR is much smaller than $R + R_1$

$$\therefore E_{AB} = \frac{E\Delta R}{R(1 + \frac{R_1}{R})^2}$$

Suppose R_{1A} changes by $+\Delta R$ and R_{1B} by $-\Delta R$

$$\therefore I_1 = \frac{E}{R + R_1 + \Delta R} \quad \text{and} \quad I_2 = \frac{E}{R + R_1 - \Delta R}$$

$$E_A = \frac{E}{1 + \frac{R_1}{R} + \frac{\Delta R}{R}} \quad \text{and} \quad E_B = \frac{E}{1 + \frac{R_1}{R} - \frac{\Delta R}{R}}$$

$$E_{AB} = E_B - E_A$$

$$\therefore E_{AB} = \frac{2\,\frac{\Delta R}{R}\,E}{(1 + \frac{R_1}{R} + \frac{\Delta R}{R})(1 + \frac{R_1}{R} - \frac{\Delta R}{R})}$$

$$= \frac{2\,\frac{\Delta R}{R}\,E}{(1 + \frac{R_1}{R})^2 - (\frac{\Delta R}{R})^2}$$

But $(\frac{\Delta R}{R})^2$ is much smaller than $(1 + \frac{R_1}{R})^2$

$$\therefore E_{AB} = \frac{2E\,\Delta R}{R\,(1 + \frac{R_1}{R})^2}$$

$\therefore$ The voltage in the second case is double the voltage in the first case.

APPENDIX IV

Historic Survey of Spray Analyzers

HISTORIC SURVEY OF SPRAY ANALYZERS

A few of the most successful methods which have been developed for the analysis of fuel sprays are outlined below.

Visual Observation:

The simplest method used for studying the spray uniformity as it leaves the nozzle is examination with the naked eye. It is the first step in the routine testing of nozzles and, with a little experience, this method gives fairly reliable results.

The Patternator:

The most common method now in use for quick analysis of fuel sprays and comparison of nozzles is the so-called "patternator". Basically, this device is a compartmented circular pan centered under the nozzle at some arbitrary distance away. The pan is divided radially and concentrically into triangular center compartments and trapezoidal outer compartments. Each compartment has its own drain into a burette, with a mechanism to divert the drains from all compartments into or away from all burettes simultaneously. Comparison of the amount of liquid collected in each compartment during the test interval gives the uniformity and relative mass distribution of the spray with a precision proportional to the number of compartments.

Sampling:

Microscope slides or plates are used as sampling devices to collect drops from the spray. These slides or plates are coated with suitable material so that the drops intercepted can be counted and measured. In some cases the slide is coated with a substance not wetted by the sprayed fuel, thus maintaining the drops in a near-spherical shape until they are photographed. The negative can then be enlarged and the images of the drops measured. The uniformity of the spray can be studied by introducing the sampling slide or plate in different positions in the spray.

The Electrostatic Counter:

This method makes use of the fact that small particles in a stream carry electronic charges proportional to their surface area. A sample of the spray is drawn at high velocity through a pipe and is allowed to pass through a tapered orifice and impinge upon a charged wire. The wire is connected through amplifiers to an electronic counter which records the number and amplitude of the pulses created by the discharge from the spray particles to the wire. The magnitude of the pulse has been shown by Guyton to be proportional to the surface area of the drop. This method is used for different sprayed liquids and appears to be promising.

Light Scattering:

A point source of light seen through the spray appears to have a ring corona whose average diameter is a function of the

predominant drop size in the spray. The breadth of the corona, or secondary coronas, is a function of the range of the drops in the spray. The intensity of the light scattered at right angles to a beam passing through a spray is measurable by a photocell, and can be calibrated against the number of drops. The decrease in light transmission through a spray may be measured and calibrated to correspond to numbers of drops of given sizes.

Photographing:

This is the most recent method for studying spray characteristics which was devised by York in his work at the University of Michigan. In this method, photographs are taken with a special camera with an exposure time of 8 micro-seconds, at adjacent points in the spray, until the spray is sufficiently sampled. Counting and measuring the drop images provide data for calculating drop size distribution curves and average drop diameter. One advantage of this method is that there is no sampling device to interfere with the spray. However, this method takes a long time to carry out. It is, therefore, not suitable for a rapid analysis of fuel sprays.

BIBLIOGRAPHY

1. Arenberg, D. L.

"Determination of Icing Conditions for Airplanes" Transactions, National Research Council of the American Geographical Union, 1943, Part 1, pp. 99-122.

2. Clapp, C. W.; Bernstein, S.

"Noncontacting Thickness Gauge Using Beta Rays" Electrical Engineering, April, 1950, pp. 308-310.

3. De Juhasz, K. J.

"Some Notes on the Use of the Optical Indicator" Automobile Engineering, London, Vol. 39, 1939, pp 317-319

4. Dema Laboratory

"Laboratory Equipment for Testing and Research Work on Diesel Engines" Dema Laboratory Equipment Bulletin, No. 2, Diesel Engine Manufacturers Association.

5. Drinker, P.

"An Alternating Current Precipitator for Sanitary Air Analysis - An Inexpensive Precipitator Unit" Journal of Industrial Hygiene, Vol. 41, no. 10, 1932, pp. 364.

6. Guyton, A. C.

"An Electronic Counting and Size Determination of Particles in Aeorsols" Journal of Industrial Hygiene, Vol. 28, no. 4, July, 1946, p. 133.

7. Hatch, T., Warren, L., and Drinker, P.

"Modified Form of Greenberg-Smith Impinger for Field Use, With a Study of its Operating Characteristics" Journal of Industrial Hygiene, Vol. 14, no. 8, 1932, p. 301.

8. Hicks, C. W. and Moore, C. S.

"The Determination of Several Spray Characteristics of a High Speed Oil Injection System with an Oscilloscope" National Advisory Committee for Aeronautics Technical Note, no. 298.

9. Kuehn

"Atomization of Liquid Fuel" I, II, III, National Advisory Committee for Aeronautics Technical Memos, 329, 330, 331., 1930

10. Langmuir, I. and Blodgett, K. B.

"A Mathematical Investigation of Water Droplet Trajectories" U.S. Army Air Forces Technical Report, no. 5418, 1946

11. Matthews, R.

"Discharge Characteristics of a High Speed Fuel Injection Engine" National Advisory Committee for Aeronautics Technical Memo, no. 213, 1925

12. May, K. R.

"The Cascade Impactor: An Apparatus for Sampling Solid and Liquid Particulate Clouds" The Proton Report, no. 2463, Dec. 8, 1942.

13. Muraszew, A.

"Fuel Injection in Internal Combustion Engines. Fuel Spray Phenomena" The Motor Industry Research Association (Great Britain) Report no. 1947/R/G.

14. Neuberger, H.

"Notes on Measurement of Rain Drop Sizes" Bulletin of The American Meteorological Association Vol 23, 1942, pp. 274-276.

15. Nielson, D. M

"Electric Strain Gauges" Electronics, Dec. 1943, p.106

16. Orent, E.

"Jet Nozzle Testing" University of Michigan Conference on Fuel Sprays, Ann Arbor, March 30-31, 1949

17. Perry, J. H.

"Chemical Engineering Handbook" (second edition) McGraw-Hill, p. 445.

18. Probert, R. P.

"The Influence of Spray Particle Size and Distribution in the Combustion of Oil Droplets" Philosophical Magazine, London. Vol 37, 1946, pp. 94-105.

19. Rothrock, A. M. and Waldron, C. D.

"Some Characteristics of Fuel Sprays at Low Injection Pressures" National Advisory Committee for Aeronautics Technical Memo no. 399, 1931.

20. Rupe, J. H.

"A Technique for the Investigation of Spray Characteristics of Constant Flow Nozzles" University of Michigan Conference on Fuel Sprays, Ann Arbor, March 30-31, 1949.

21. Sauter, J.

"Determining the Size of Drops in Fuel Mixtures of Internal Combustion Engines" National Advisory Committee for Aeronautics Technical Memo no. 390, 1926.

22. Schmidt, J. M.

"Measurement of Droplet Sizes by the Diffraction Ring Method" Jet Propulsion Laboratory of the California Institute of Technology Progress Report, no 3-18, July 27, 1948.

23. Schweitzer, P. H.

"Oil Spray Research at the Pennsylvania State College Proceedings at the First Oil Power Conference", Pennsylvania State Technical Bulletin, no. 5, 1929, pp. 65-70, pp. 175-188.

24. Stoker, R. L.

"A Method of Determining the Size of Droplets Dispersed in a Gas" Journal of Applied Physics Vol. 17, April, 1946.

25. Tolman, R. C. and Reyerson, L. H.

"An Electrical Precipitator for Analyzing Smokes" Journal of the American Chemical Society Vol. 4 no. 587, 1919.

26. Wells, P. V. and Gerke, R. H.

"An Oscillation Method for Measuring the Size of Ultra-microscopic Particles" Journal of the American Chemical Society Vol 41, March, 1919.

27. Wilson, J. G.

"Notes on Optical Methods of Measuring the Size of Small Water Drops" Proceedings of the Cambridge Philosophical Society, (England) Vol. 32, 1936.

28. York, J. L.

"Photographic Analysis of Sprays" University of Michigan PhD Thesis, 1949.

PICTURES



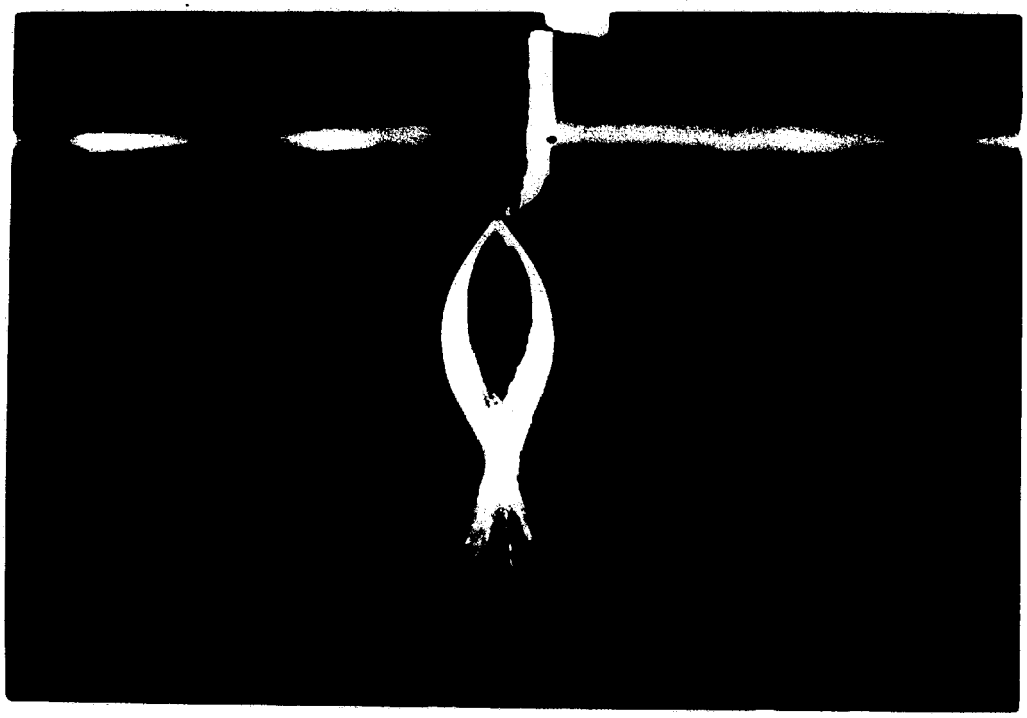

PICTURE (1)
PRESSURE 25 PSI

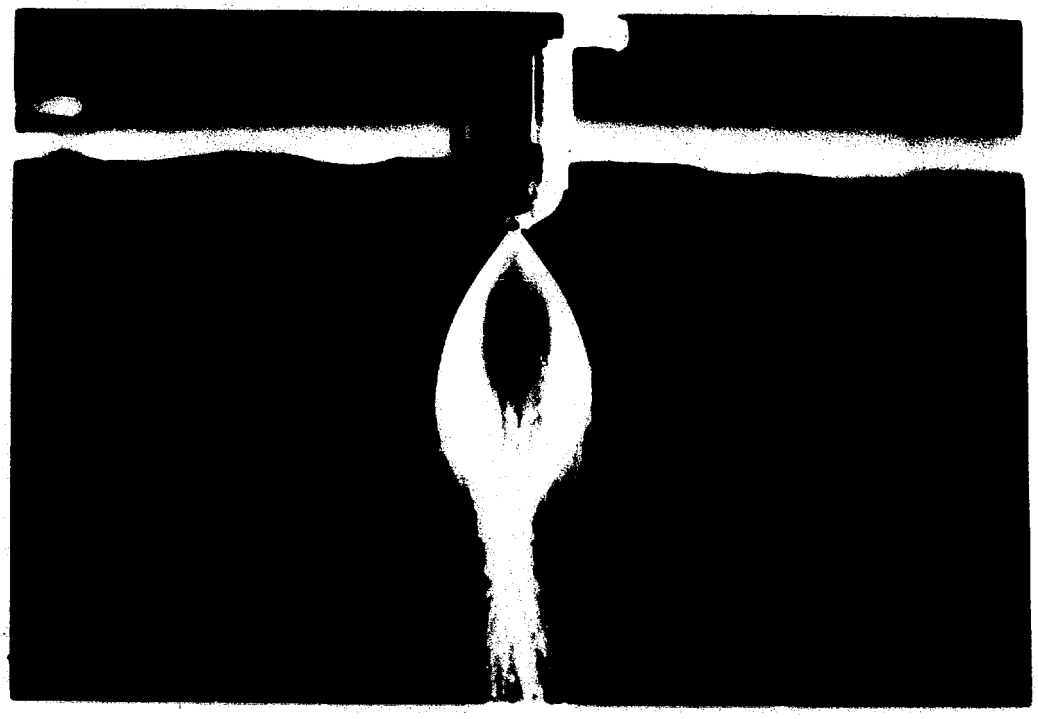

PICTURE (2)
PRESSURE 50 PSI

FLOW OF TYPICAL SIMPLEX NOZZLE (6702074 A 4-2/3 DED C52)

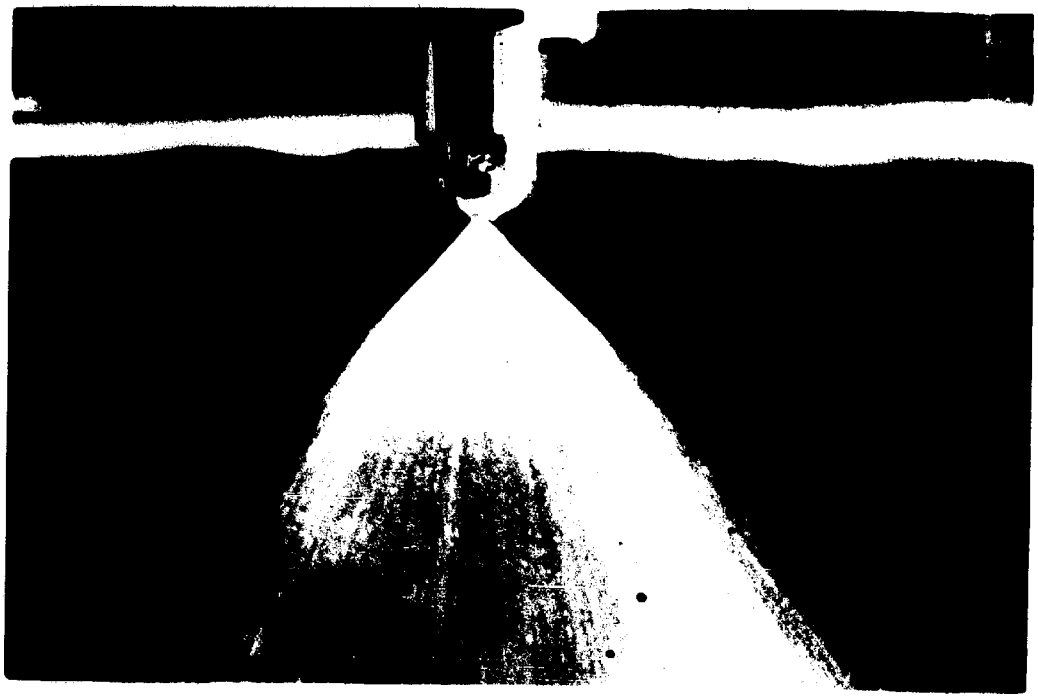

PICTURE (3)
PRESSURE 75 PSI



PICTURE (4)
PRESSURE 100 PSI

FLOW OF TYPICAL SIMPLEX NOZZLE (6702074 A 4-2/3 DED C52)



PICTURE (5)
PRESSURE 200 PSI



PICTURE (6)

PRESSURE 300 PSI

FLOW OF TYPICAL SIMPLEX NOZZLE (6702074 A 4-2/3 DED C52)

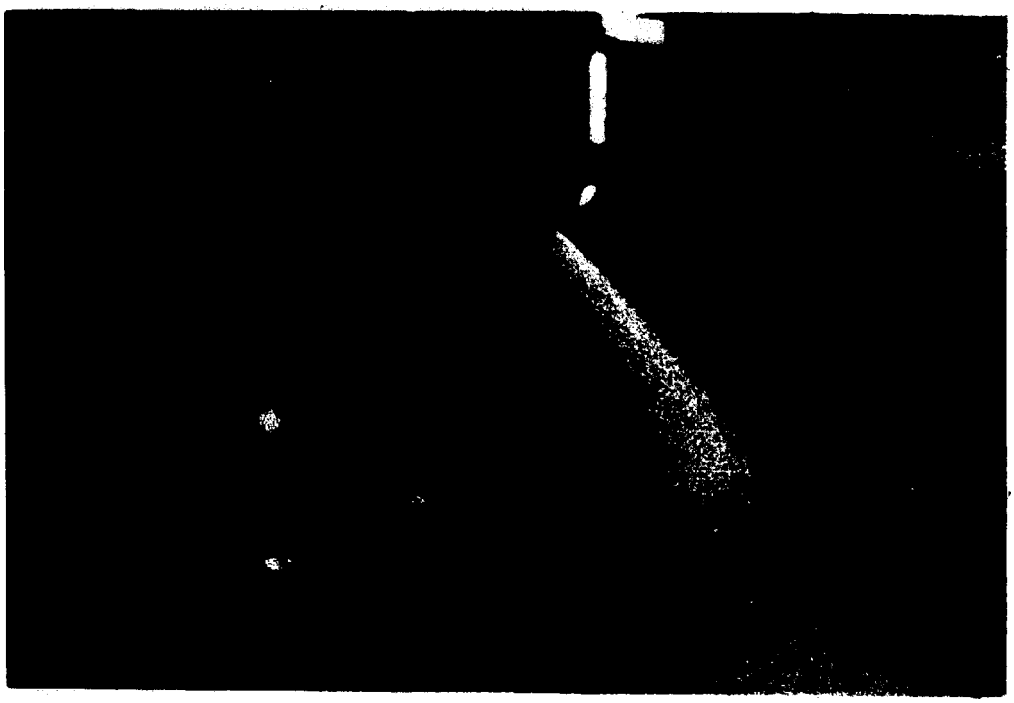

PICTURE (7)
PRESSURE 400 PSI

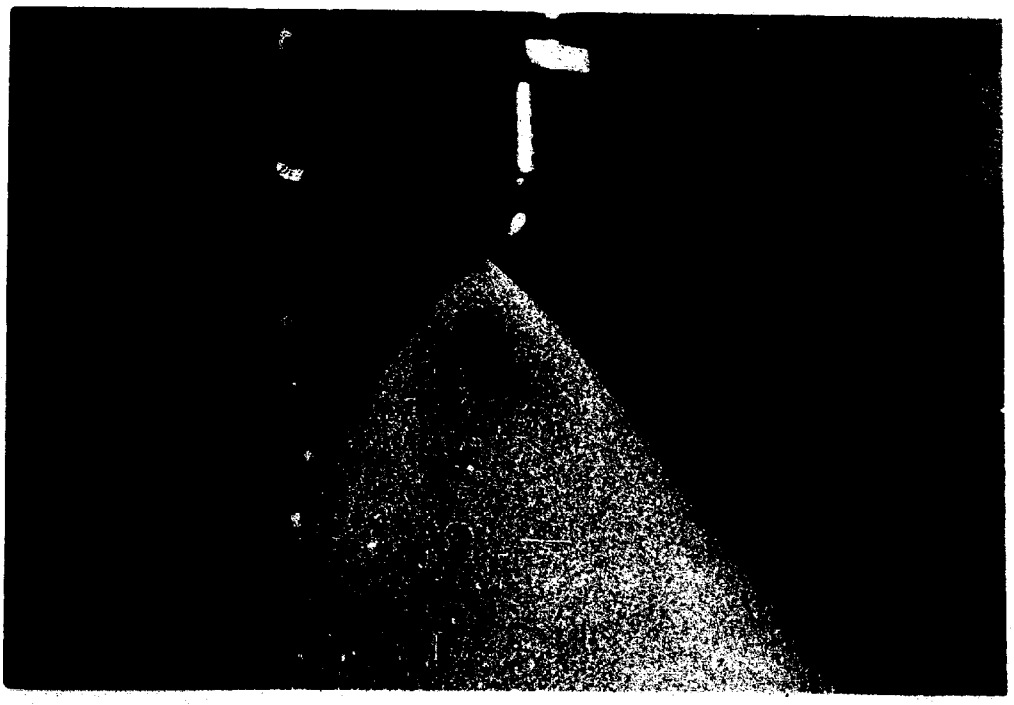

PICTURE (8)
PRESSURE 500 PSI

FLOW OF TYPICAL SIMPLEX NOZZLE (6702074-A 4-2/3 DED C52)



PICTURE (10)

PRESSURE 100 PSI

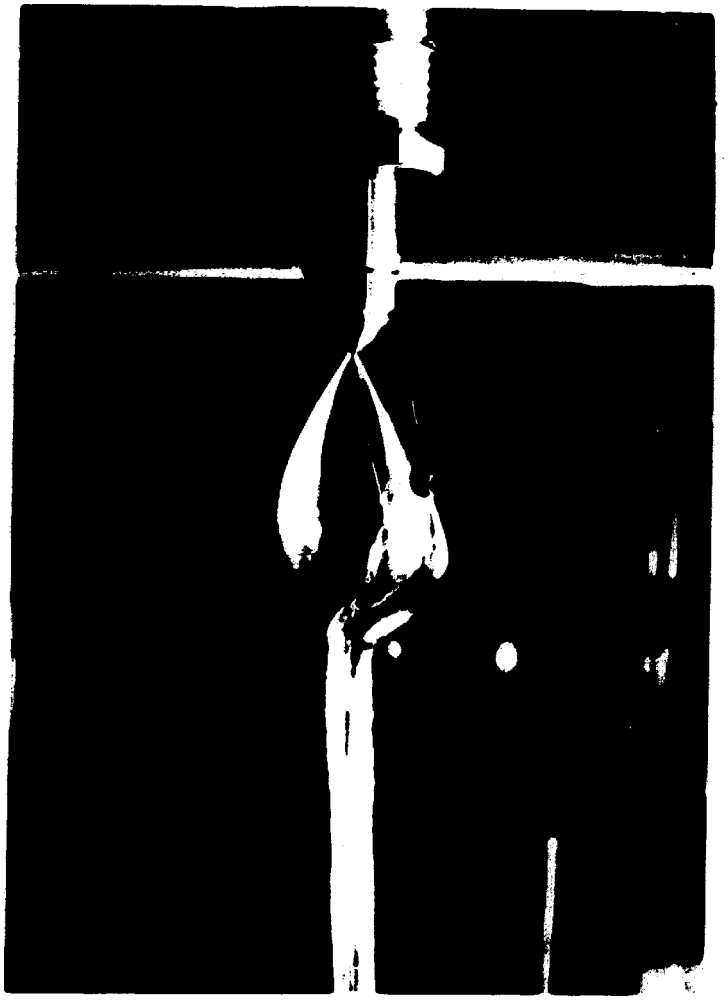

PICTURE (9)

PRESSURE 25 PSI

SLENDER CUPRO-NICKEL WIRE PICK-UP ON GLASS SUPPORTS

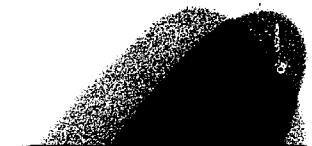



PICTURE (11)

ORIFICE OF DEFACED MONARCH SIMPLEX NOZZLE

(6702074-A 3-29-48 5 DED C-52)

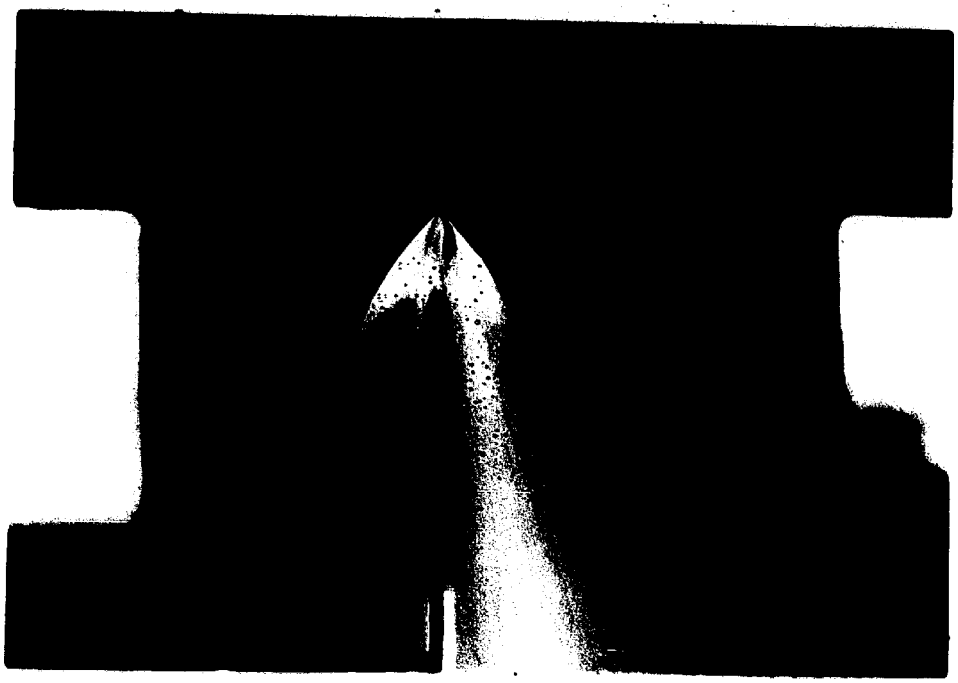

PICTURE (12)
PRESSURE 50 PSI

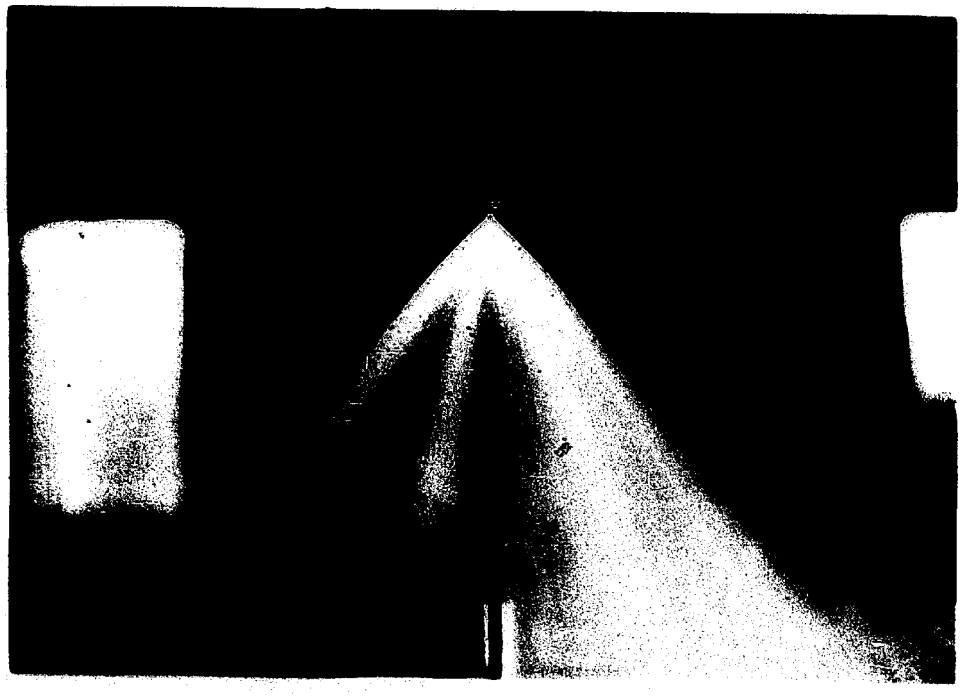

PICTURE (13)

PRESSURE 100 PSI

FLOW OF (DEFACED) NOZZLE (6702074 A 3-29-48 5 DED C-52)

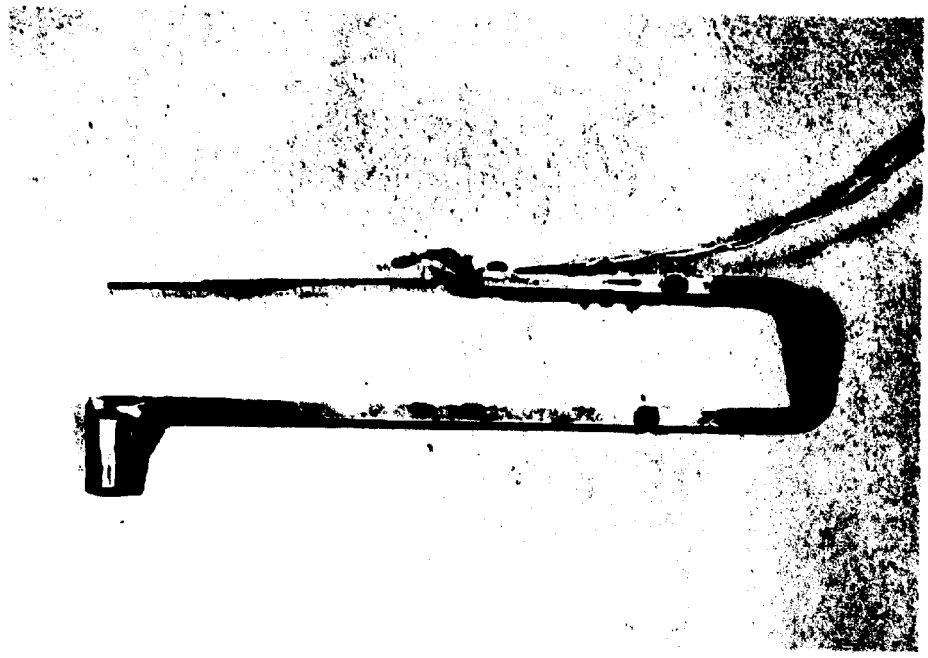

PICTURE (14)
BRACKET CARRYING CANTILEVERED BEAM

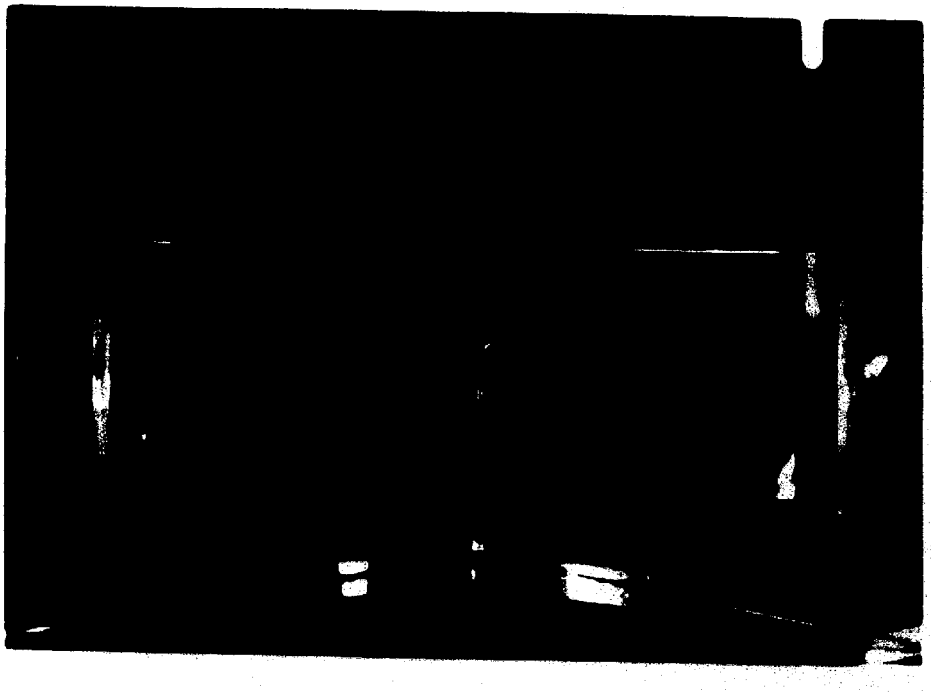

PICTURE (15)

MOUNTING OF STRAIN GAUGE PICK-UP

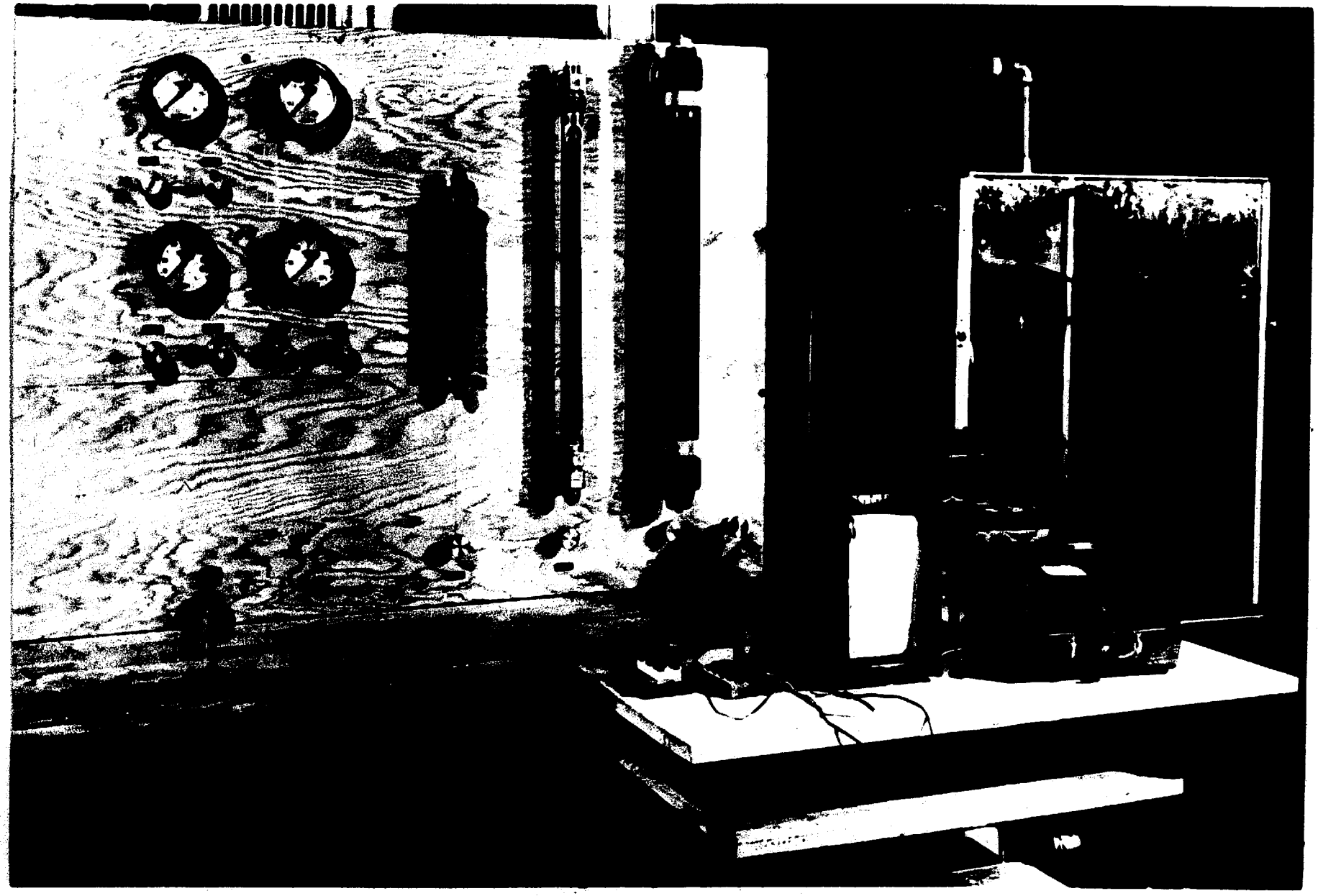

PICTURE (16)

PANEL AND SPRAY CHAMBER

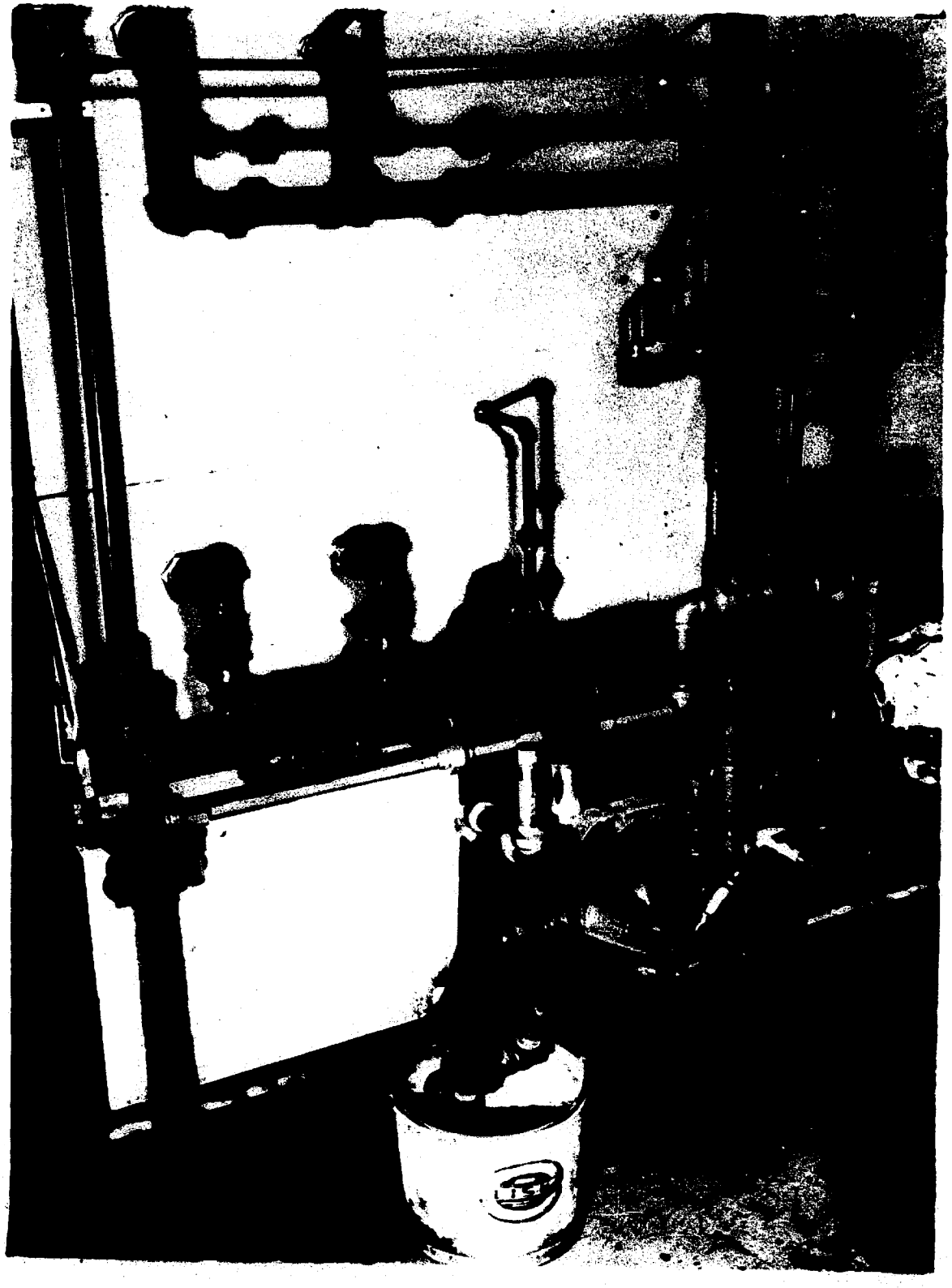

PICTURE (17)

PIPING SYSTEM BETWEEN PUMPS AND NOZZLE

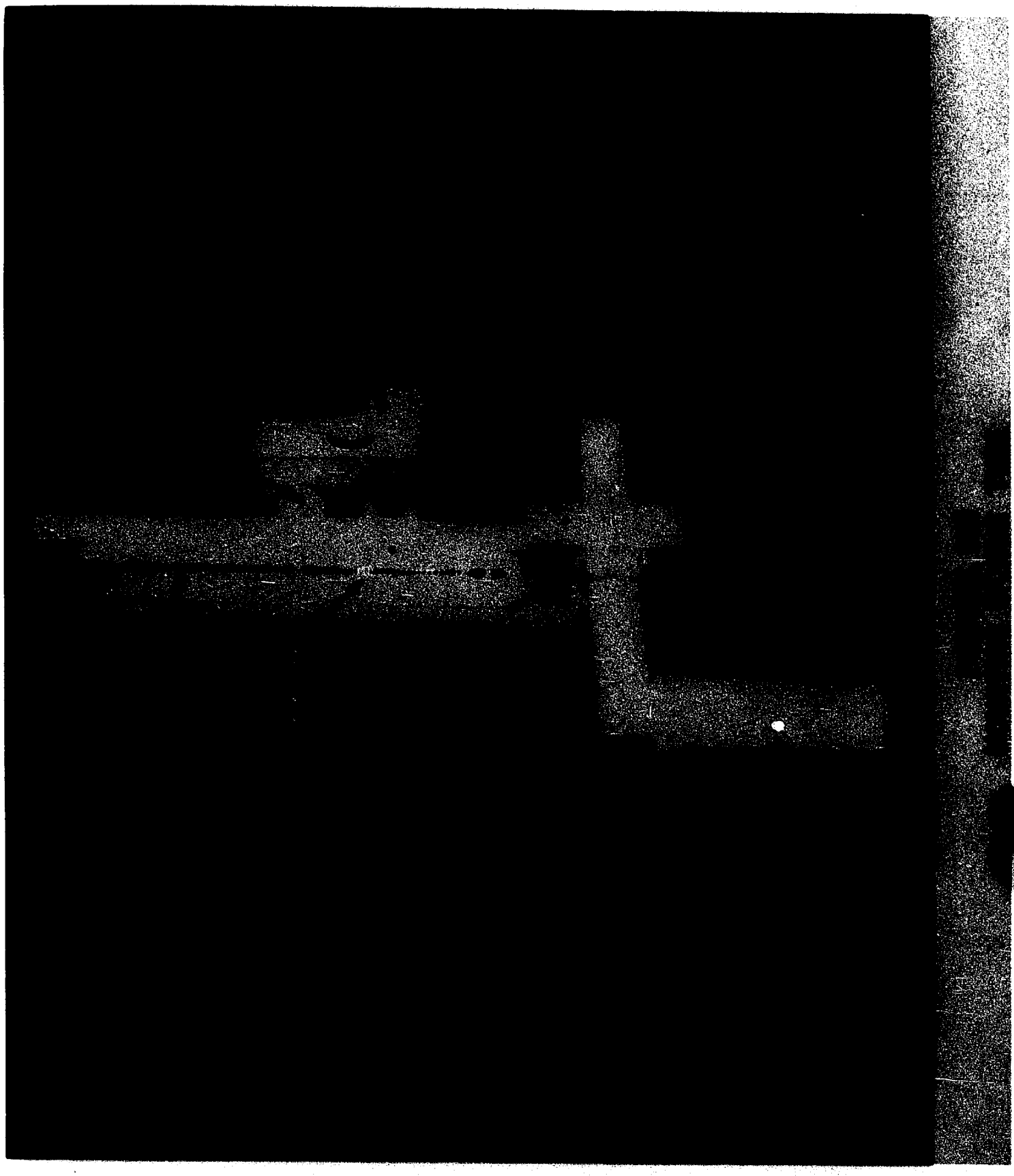

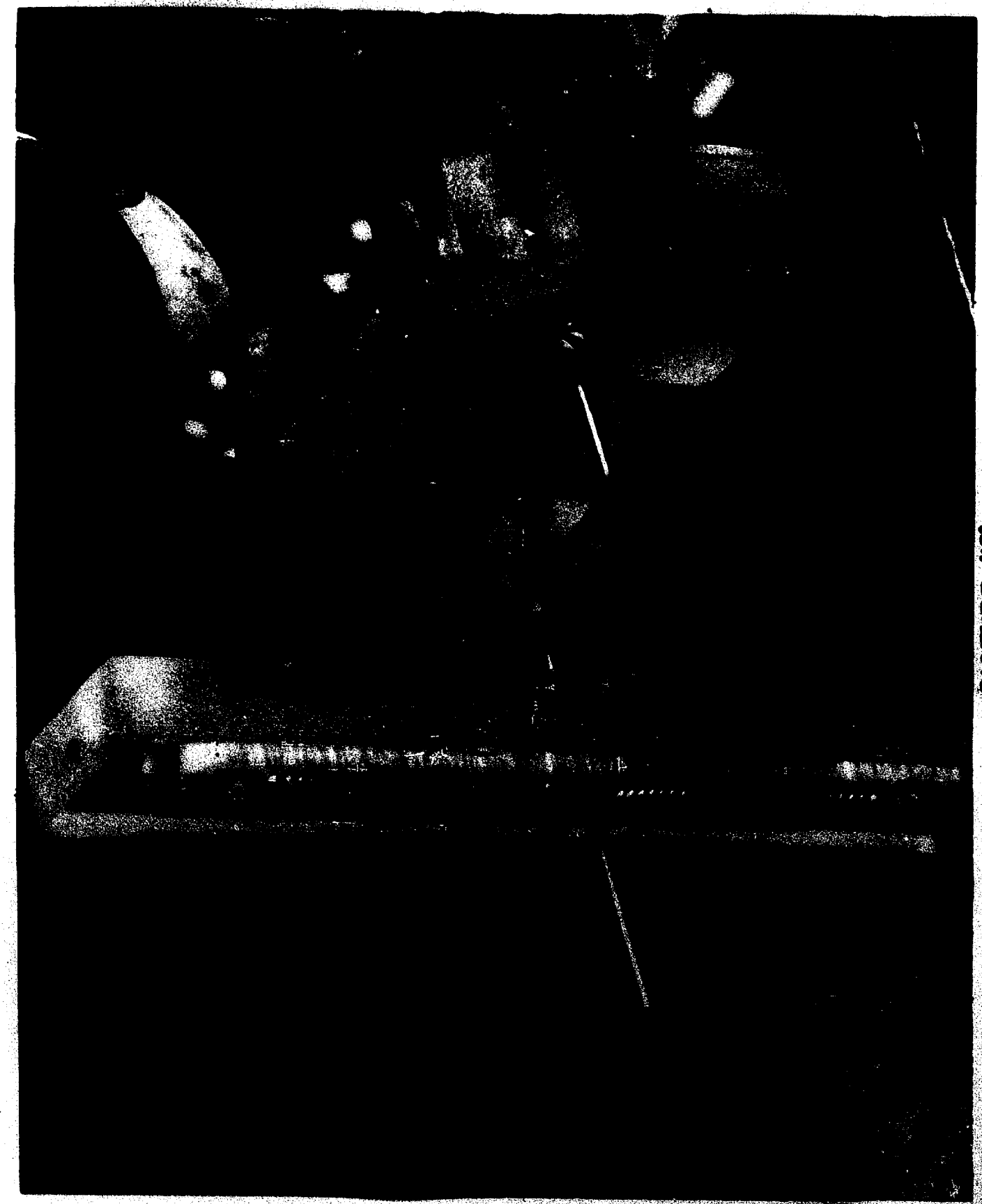

PICTURE (19)
MOUNTING OF TWO TUBES